

This dissertation has been 63-4513
microfilmed exactly as received

PALMER, James Daniel, 1930-
AN INVESTIGATION OF SPONTANEOUS ELECTRO-
MAGNETIC EMISSION FROM STATIC PLASMAS.

The University of Oklahoma, Ph.D., 1963
Engineering, electrical

University Microfilms, Inc., Ann Arbor, Michigan

THE UNIVERSITY OF OKLAHOMA

GRADUATE COLLEGE

AN INVESTIGATION OF SPONTANEOUS ELECTROMAGNETIC
EMISSION FROM STATIC PLASMAS

A DISSERTATION

SUBMITTED TO THE GRADUATE FACULTY

in partial fulfillment of the requirements for the

degree of

DOCTOR OF PHILOSOPHY

BY

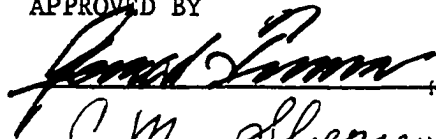
JAMES DANIEL PALMER

Norman, Oklahoma

1963

AN INVESTIGATION OF SPONTANEOUS ELECTROMAGNETIC
EMISSION FROM STATIC PLASMAS

APPROVED BY



C. M. Shepovich

Sybrand Proeme

George M. Lewis

Raymond A. Daniels

DISSERTATION COMMITTEE

ACKNOWLEDGEMENT

The author wishes to express his sincere gratitude to the many individuals from whom assistance has been obtained in the preparation of this thesis. In particular, appreciation is extended to Dr. A. von Engel, of Oxford University, for originally suggesting the problem area, and to Professor Gerald Tuma, Chairman of the School of Electrical Engineering at the University of Oklahoma, under whose guidance and council this program was performed.

The advice and suggestions of Dr. J. A. Nickel, Chairman, Mathematics Department, Oklahoma City University, and Mr. D. R. Williams, of the School of Electrical Engineering of the University of Oklahoma, proved to be invaluable during certain phases of the program and are sincerely appreciated. Thanks are also extended to the various members of the Doctoral Advisory Committee for their interest in this work.

Finally, thanks are to be extended to the Streeter-Amet Division of Goodman Manufacturing Company for their financial support in the form of supplying certain specialized pieces of electronic equipment.

TABLE OF CONTENTS

	Page
LIST OF TABLES.....	v
LIST OF ILLUSTRATIONS.....	vi
Chapter	
I. INTRODUCTION.....	1
II. STATEMENT OF THE PROBLEM AND REVIEW OF PREVIOUS WORK.....	6
III. DESCRIPTION OF EXPERIMENTAL APPARATUS.....	16
IV. PROCEDURE.....	24
V. THEORY.....	30
VI. RESULTS.....	59
VII. CONCLUSIONS.....	86
VIII. RECOMMENDATIONS.....	88
BIBLIOGRAPHY.....	90
APPENDICES	
A. VOLT-AMPERE CHARACTERISTICS OF THE GLOW-DISCHARGE TUBE.....	96
B. METHODS OF PRODUCING RADIATION BY ACCELERATING CHARGES.....	101
C. RECURRENCE RATE DATA.....	112

LIST OF TABLES

Table		Page
1	Variation of Relative Amplitude and Decay Time (Exterior Probe).....	70
2	Variation of Signal Level as a Function of Position Along the Tubes.....	73
3	Correlation Coefficient Calculation Data.....	80
4	Recurrence Rate Summary.....	81
5	Recurrence Rate Data.....	113
6	Summary of Reduced Recurrence Data.....	115

LIST OF ILLUSTRATIONS

Figure Number		Page
1	Line Diagram of Experimental Apparatus.....	17
2	End Plug and Electrode Support Configuration.....	19
3	Photograph of Test Section.....	20
4	Microwave Diagnostic Equipment.....	23
5	Plasma Tube Volt-Ampere Characteristic.....	26
6	Typical Probe Waveshape	29
7	Glow Discharge Features.....	32
8	Cathode Fall Region Voltage.....	34
9	Geometry of the Cylindrical Glow.....	36
10	Accelerating Charge Geometry.....	42
11	Idealized Cathode Fall Region Waveshape.....	50
12	Diagram of Possible Cathode Fall Excitation Mechanism.....	52
13	Interferometer Waveshape.....	60
14	Interior Probe Waveshape.....	62
15	Exterior Probe Waveshape.....	62
16	Time Constant Determination for Interior Wave.....	63
17	Amplitude Variation at the Interior Probe.....	66
18	Exterior Probe Waveshape.....	67

19	Variation of Amplitude and Decay Time at the Exterior Probe.....	69
20	Exterior Probe Amplitude Variation.....	72
21	Amplitude Variation for Shielding Along the Tube.....	74
22	Time Constant Determination for Air and Argon.....	77
23	Interior Probe Recurrence Rate.....	78
24	Exterior Probe Recurrence Rate.....	79
25	Recurrence Rate Comparison.....	83
26	Plasma Tube Characteristics.....	97
27	Plasma Tube Characteristics.....	98
28	Plasma Tube Characteristics.....	99
29	Plasma Tube Characteristics.....	100
30	Cerenkov Radiation Geometry.....	108

AN INVESTIGATION OF SPONTANEOUS ELECTROMAGNETIC
EMISSION FROM STATIC PLASMAS

CHAPTER I

INTRODUCTION

The field of gaseous electronics represents a domain in which a continuous research effort has taken place over the past one-hundred and fifty years. The first investigations were concerned with arcing between points of high potential, while the modern aspects are generally thought of under the title plasma physics. Within the confines of plasma physics, effort is devoted to the furtherance of understanding of fundamental processes, investigation of new anomalies, and in development of theories and techniques into product design. The range of problem areas in this field is best demonstrated by noting that studies cover such diverse topics as the nature of secondary processes in gaseous discharges and the communication blackout that occurs during re-entry due to the plasma sheath that surrounds the re-entering vehicle.

The program of work described in this dissertation was generally intended as one which would relate certain aspects of fundamental processes that take place in gaseous discharges to the experimental work in the communications problem. This experimental

work most generally utilizes as an experimental medium, the normal glow region of the gaseous electronic discharge, while the problem areas considered in the greatest detail are those related to propagation. Thus, if a signal is to be propagated through an ionized medium, knowledge of the possible modifications that can be exerted by the medium must be found. An incident wave to be transmitted through an ionized region can be expected to suffer such deleterious effects as phase shift, attenuation, intermodulation, cross-modulation, and electrical parameter changes. In addition to the aforementioned interactions there is the possibility of the media itself contributing a measure of energy to the signal. It is in this latter area that a bridging of the fundamental to the applied is hoped to bear some significance.

The specific area of interest has been centered around the ionized medium and some of the immediate problems associated with this restricted region of interest. Among the many active researchers in this same general area are Chodorow and Kino (5), Bachynski (1), Drummond (8), and Flock and Elliott (12). Chodorow and Kino are attempting to define plasma sheath parameters in an effort to learn more concerning the interaction of incident electromagnetic energy on plasmas. In their most recent progress report on plasma boundary layer studies (5), the following is presented in Section 2, Probe and Discharge Theory.

"In view of the situation outlined above (inaccuracies in plasma equations), it seems desirable to obtain rigorous solutions to the full plasma-sheath equation. Unfortunately, even for the case of plane geometry, a full analytic treatment has yet to be demonstrated and we must resort to numerical computation.

.....Such solutions (ed) are more relevant to the experimental program in progress to measure the steady potential as well as any high frequency oscillations in the sheath."

To date, they report little success in expressing their observations and theories analytically. In addition, experimental difficulties have caused concern, particularly the interaction of their electron beam probes and the plasma sheath. Bachynski relates a number of the areas of concern, and presents some of the difficulties that have been or may be experienced. His own experimental program has progressed well and his group has reported a new microwave measuring technique which they have developed to obtain simultaneous measurements of propagation parameters. Elliott's work has pointed up the need for more information relating basic properties to various aspects of propagation. Measurements performed in his laboratory dealing with microwave transmission properties of plasmas showed a poor correlation coefficient between experiments and, in addition, between proposed theory and experiment. The degradation of the signal through the plasma is clearly evident from oscilloscope tracings and, a number of fluctuations in the traces are not explained, which could have an effect on propagation.

Since the majority of work on propagation through plasmas is performed on a laboratory scale with laboratory plasmas, it is essential to know as much as possible about the electromagnetic characteristics of the medium. A number of good texts and articles (9, 14, 19, 27) deal extensively with the complex dielectric constant of such a medium and present numerical solutions in both tabular and curve form. Of more immediate interest, however, is the manner in which the plasma

itself might contribute as an active source. Again, a great deal of information is available in both book and article form (9, 20, 24, 25), which contain sections on such phenomena as cyclotron resonance, Bremstrahlung, Cerenkov, and other ways in which a signal may be generated. In addition, the entire field of magnetohydrodynamics presents such possible wave modes as Alfvén, acoustic, and other MHD waves. Thus, a wealth of information is available on many possible wave modes in plasmas.

None of the above presentations has supplied an answer to a more immediate problem. This was the occurrence of a voltage spike on the modulated wave detected by a microwave interferometer used to measure phase shift of an incident wave through a plasma. A preliminary investigation revealed this voltage spike to be some two orders of magnitude greater than the signal from the microwave source. Further, the amplitude of the signal had a direct relationship with the plasma tube current. It was decided to investigate this signal in some detail to determine if it could be related to some basic property of the gaseous discharge. A thorough investigation revealed many instances of signals that could not be accounted for, but no generally accepted treatment was found relating these signals to some phenomena in the gas.

The present program has thus evolved from a desire to gain more knowledge concerning fundamental properties of gaseous electronic discharges and the more immediate, short-range goal of explaining a signal that has caused great concern and most probably erroneous readings in other experimental areas. It was felt that if a consistently good

job of design and development is to be performed on electromagnetic systems that operate in the presence of ionized gases, more knowledge pertaining to the spontaneous electromagnetic emission from the research medium is mandatory.

The purpose of this investigation is to study the electromagnetic emission characteristics of gaseous plasmas in the VHF, UHF and microwave spectral regions and attempt to relate this information to the fundamental processes involved in these discharges.

CHAPTER II

STATEMENT OF THE PROBLEM AND REVIEW OF PREVIOUS WORK

Objectives of the Study

Spontaneous electromagnetic emission from static plasmas has long been recognized as being generated by fundamental processes in the plasma itself. Knowledge of the explicit processes and conditions giving rise to this electromagnetic radiation is lacking in both the far infrared and microwave regions of the spectrum. In particular, knowledge relating to the energy loss due to accelerating charges is either missing or of a doubtful nature. If the emission characteristics of the plasma can be determined and the fundamental processes involved in some way ascertained, the static gaseous plasma will become a more useful research medium for the investigation of the interaction with active sources both from within and without.

For the communications engineer the spontaneous electromagnetic emissions are simply noise, where noise is meant to include any undesirable signal that does not contain original information intended for use. This noise could emanate from any component of a particular transmission system including in this case the plasma column, pre-amplifiers, and lead induction to name a few. If the "noise" generated by the medium itself were known, more meaningful results of

propagation effects and interaction of the medium with electromagnetic waves could be attained. Hence, the objectives of the present study involve obtaining relationships between the noise level and the characteristics of the generating medium.

The theoretical approach requires the solution of sets of non-linear, partial differential equations with variable coefficients. To obtain a solution of equations of this type requires a digital computer with a large memory capacity and a capability of high-speed calculations.

The experimental approach requires the use of a plasma generator and measuring equipment covering several ranges of frequencies. One technique of performing the experimental work consists of enclosing a stable positive column in a static plasma tube and measuring the electromagnetic radiation generated. To be completely thorough, it is necessary to determine not only the externally radiated signal, but also the signal internal to the plasma.

Early studies (c.f. Project Sherwood (2)) concerned with the interaction of microwave energy and plasmas, indicated that the plasmas were highly reflective at surface discontinuities. This meant that any internally generated signals were reflected from the surface and trapped in the plasma interior. Recent investigations have shown that this assumption was not justified. Wharton (33) made microwave diagnostic studies of high temperature plasmas and discovered that these bodies are copious emitters of radio-frequency energy. These emissions are felt to come from cyclotron resonance rather than a black-body effect, since a simple calcula-

tion shows the black-body contribution to be greater than measured values.

The process of determining the internal emission characteristics of a static plasma column can be accomplished by insertion of a microwave pickup in the positive column. This pickup is passive and any signal generated by the medium will be picked up. The presence of the probe in the medium will cause a distortion of the plasma; however, it was felt that a measurement obtained in the center would provide information not available by other techniques.

Previous Investigations

The fields of plasma physics and electromagnetic properties of plasmas have experienced a rapid expansion in recent years. Technical journals in electrical engineering, mechanical engineering and physics have devoted special issues to this subject. In addition, a technical journal in the field of fluid dynamics utilizes a great percentage of its space for plasmas. However, this tremendous upsurge of technical material is by no means an indication of the total activity in the field and, further, the level of effort is expected to continue to climb at a rapid rate. Important work is being done by electrical engineers, physicists, chemists and others in the physical science disciplines.

It should be noted that the bulk of the work carried on can be listed in two major categories. These are the determination of the physical properties of plasmas and the effect of plasmas on microwave energy transmission. The latter category is mainly the concern of

the electrical engineer, while the former is primarily the domain of the physicist.

In spite of the great amount of work being done, very little effort has been placed on determining the microwave emission characteristics from an experimental standpoint. Most of the work involving microwave frequencies has been directly related to the problems of transmitting a radio frequency signal through the plasma. Government and industry interests in the propagation problem show a tendency to extensive empirical work in many instances, rather than performing an analysis of the pertinent basic parameters. This approach works well for ground-based laboratory experiments, but in no way suffices in the re-entry communications problem, as recent flights show (3).

Typical of recent pertinent work in this field are the investigations of Cloutier, Bachynski and Graf (6), Flock and Elliott (12), Raemer (24), Drummond (10), and Chen (3). These investigations are concerned primarily with gross effects of plasmas on incident electromagnetic waves. The work has been in the form of theoretical and experimental assessments of the propagation problem.

Cloutier, Bachynski and Graf have carried out a series of experiments to determine the influence of a plasma sheath on the radiation pattern of microwave antennas. The far field radiation pattern of the antenna was determined as a function of plasma properties. Diffraction theory was used to correlate the results to determine the influence of the various parameters. The reciproc-

ity theorem was then employed to predict the effect of the plasma on the antenna pattern. A unique measuring arrangement was developed which allows simultaneous measurement of both phase and amplitude at a very high sampling rate. This work represents a significant contribution in this field and the measurement technique developed is truly important. However, no measurements of a passive nature were made to ascertain the contribution of the medium to the signal. The plasma medium used in these studies was an alternating current helium discharge. It was noted that severe effects take place as a result of plasma relaxation time and that during steady state, noise shows on the output traces. This factor was not investigated further.

Flock and Elliott have examined the propagation of a plane wave through a plasma layer to determine both the experimental and theoretical performance of microwave horns. Their results show a loss of energy on off axis regions as compared to the same pattern in free space. The plasma used for these experiments was a modified commercial mercury vapor ignitron tube. The modification consisted of enlarging the area of the tube to be presented to the antenna. Acceptable comparison was obtained between theory and measurement, although the overall accuracy is limited by such factors as leakage currents around the walls, ratio of plasma dimensions to antenna dimensions and non-uniformities in the plasma medium. Again, no attempt was made to determine the deleterious effect of the generation of energy from within the plasma on the antenna.

The theoretical and experimental work that has been accomplished

to date has had a meaningful and significant impact on the field of propagation effects through plasmas. The investigation of the effects of plasmas on the radiation patterns of antennas, however, has not taken into consideration the contributory effects of the plasma as a source of microwave energy. Work by Tamir and Oliner (29), Wait (32), and by Newstein and Lurye (22), has all been concerned with the influence on the radiation field due to plasma sheaths of varying thicknesses. The assumptions have been that a collisionless, loss-free plasma existed and that the radiation pattern could be calculated, then correlated with the measured parameters. Results show that this strong correlation does indeed exist; however, no other factors have been considered as contributing to the measured patterns.

Hessel, Marcuvitz, and Shmoys (15) discuss the excitation of electromagnetic and acoustic waves in a plasma through coupling with an oscillating dipole current element. In their analysis they assumed the plasma to be an ideal gas with no collisions and with zero applied magnetic field. Under these assumptions they find the effects of the plasma on the far field and on optical waves. The far field is found to be unaffected. This report bears significance on the program of work reported here in that it indicates that dipole energy generated internal to the plasma will appear unaffected in the radiation zone. This signifies a direct contribution of dipole-like sources to the total field measured as in studies of propagation parameters.

Chodorow and Kino (5) are investigating the plasma sheath in

order to develop theories and techniques suitable for determining the microscopic field details. Their work takes into consideration both externally applied radio frequency and internally generated radio frequency fields due to oscillations within the plasma or within the sheath. The theoretical problem has been shown to be reducible to solving a large number of simultaneous linear algebraic equations with complex coefficients. They have found that it was necessary to develop a computer program capable of solving these equations, which is currently (November, 1962) being checked out. The experimental aspect of their work is primarily concerned with exploring the plasma sheath with an electron beam. The fields that exist are to be investigated by passing an electron beam through the sheath parallel to the sheath-plasma interface. A method of beam development and detection has been successful and deflection of the beam by small externally applied radio frequency fields has been detected through use of a specially designed silicon diode having an evaporated contact 0.003" wide. The diode is back biased and when penetrated by the electron beam, an avalanche type of amplification occurs which produces a current pulse proportional to the electron beam. The most recent progress reports by Chodorow and Kino bear out the anticipated difficulties for the theoretical work and show that the plasma equations are not well suited even for numerical solutions on computers. The main purpose of the work has been to investigate the radio frequency and direct current conditions within the sheath of a plasma. The primary problems, other than those theoretical problems previously

noted, are those of beam interaction with the plasma. These interactions can (and do) cause oscillations to be generated due to the beam itself.

Wharton (33) in the work performed at the Livermore Laboratory of the University of California, has made a thorough experimental and theoretical analysis of the microwave diagnostic techniques utilized in the measurement of plasma parameters in the thermonuclear research program. The program was aimed at determining these parameters by measuring the effect of the plasma on such microwave properties as attenuation, phase shift and reflection coefficients. While making the measurements an attempt was made to experimentally separate the signal from the noise. In addition to the usual microwave interferometer a separate receiving horn was utilized to beat out the noise from the signal. These measurements were made in the far field of the noise horn using high density plasmas. The electromagnetic emanations have proved useful in relating electron density and temperature. Wharton reports that knowledge of explicit processes and conditions contributing to radiation in the far infrared and microwave spectral regions is lacking.

Numerous theoretical studies have been made concerning the microwave properties of plasmas, but no direct measurements of the emission properties internal to the medium have been performed. Chen (4), in 1962, reported on the non-linear electrical conductivity of ionized gases and Haus (15), in 1955, presented a discussion on the noise in electron beams. Many others, including Trivelpiece (30) and Hodara (18) have reported on propagation

parameters and the difficulties found. None have attempted to ascertain the relative role played by spontaneous emissions of the plasma in their work.

Past efforts have placed considerable stress on the theoretical and experimental analysis of the effects of plasmas on the transmission of microwave signals. Some theoretical, but very little experimental work, has been performed to determine the internal emission characteristics of the medium.

Specific Objectives of the Present Investigation

The successful transmission of information on high frequency carriers through a plasma region is one of the most serious problems facing communication engineers working on space communications systems. The majority of this work is carried on either theoretically or by laboratory scale experiments. The major objective of these studies is to determine the best way to obtain transmission as a function of plasma parameters.

Several different methods are used to determine the plasma characteristics. The experiments, however, are generally of the same nature and the experimental set-up utilized in the present work is similar to that employed by other researchers. The major differences lie in the placement of the detecting probes, the data sought, and the interpretation of the results.

The present investigation was directed towards the determination of the emission characteristics of static plasmas internal to the medium itself. In addition, simultaneous measurements were made to determine these parameters external to the medium. The results

would be compared and in this manner a measure of the internal characteristics would be obtained. It was hoped that these measurements, in addition to providing more information in the field of microwave properties of plasmas, would allow a more significant interpretation of available data.

Finally, it was hoped that this study would contribute some measure of knowledge and give a small insight on the behavior of plasmas in relation to incident microwave energy, and to give some further insight on fundamental processes in gaseous discharge phenomena.

CHAPTER III

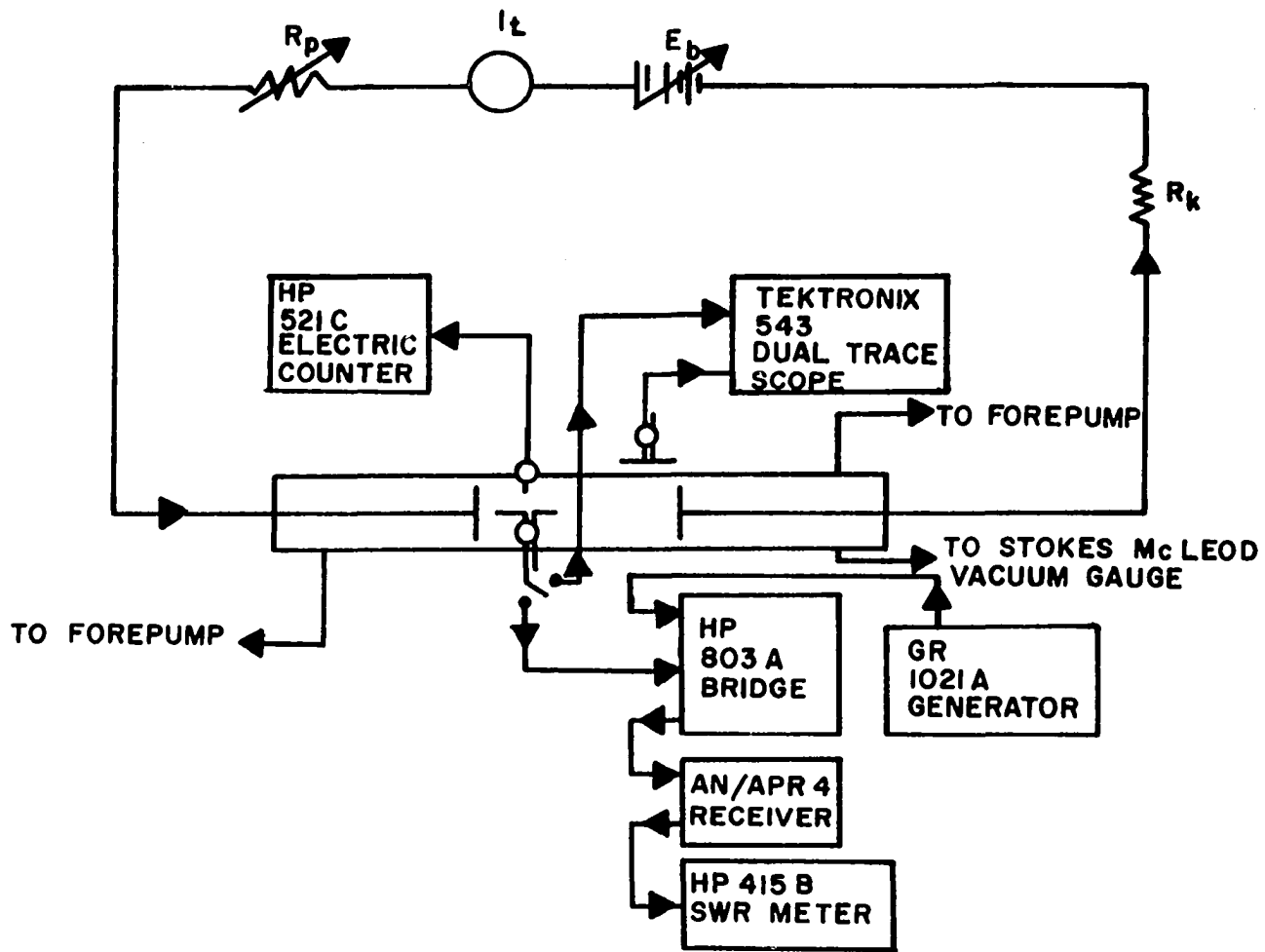
DESCRIPTION OF EXPERIMENTAL APPARATUS

The experimental apparatus consisted primarily of the following: (a) a test section (a continuous positive column plasma with variable current, pressure and distance), (b) a high voltage power supply, (c) a vacuum system, (d) various measuring, controlling and recording instruments, (e) microwave diagnostic equipment, (f) electromagnetic pickup probe for near field and for far field radiation measurements. A line diagram of the experimental apparatus in a typical configuration is shown in Figure 1.

Test Section

The test section consisted of a continuous, stable positive column plasma equipped with provisions for externally varying pressure, distance and current density. The volume available in the test section is defined by the existence of physical boundaries in the form of the tube wall and the electrodes. The inside diameter of the test section was three and one-half inches, while the maximum length was four and one-half feet.

The design particulars of the test section include the requirement to be able to vary the length of the test section during the performance of an experiment. This was accomplished through the design



17

LINE DIAGRAM OF EXPERIMENTAL APPARATUS

FIGURE 1

of the end plugs and the electrode support structure. A drawing of the end plug and accompanying electrode support structure is shown in Figure 2. The manner in which the distance between electrodes is varied is evident from this drawing. The inner seal is provided by compressing the O-rings on the support rod to hold the vacuum. The end plug itself is sealed in a like manner, but is independent of the inner plug with regard to movements.

The electrodes are connected to the support rod by means of a threaded nut attached to the electrode. This provides the desirable versatility of using different electrodes and allows ease of cleaning and polishing if they should become contaminated. Several electrode configurations were available for use.

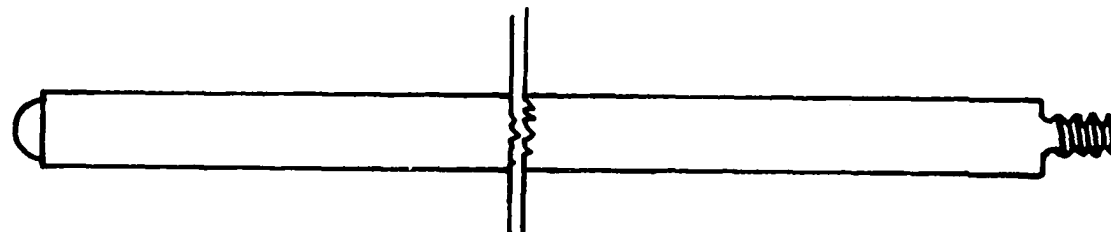
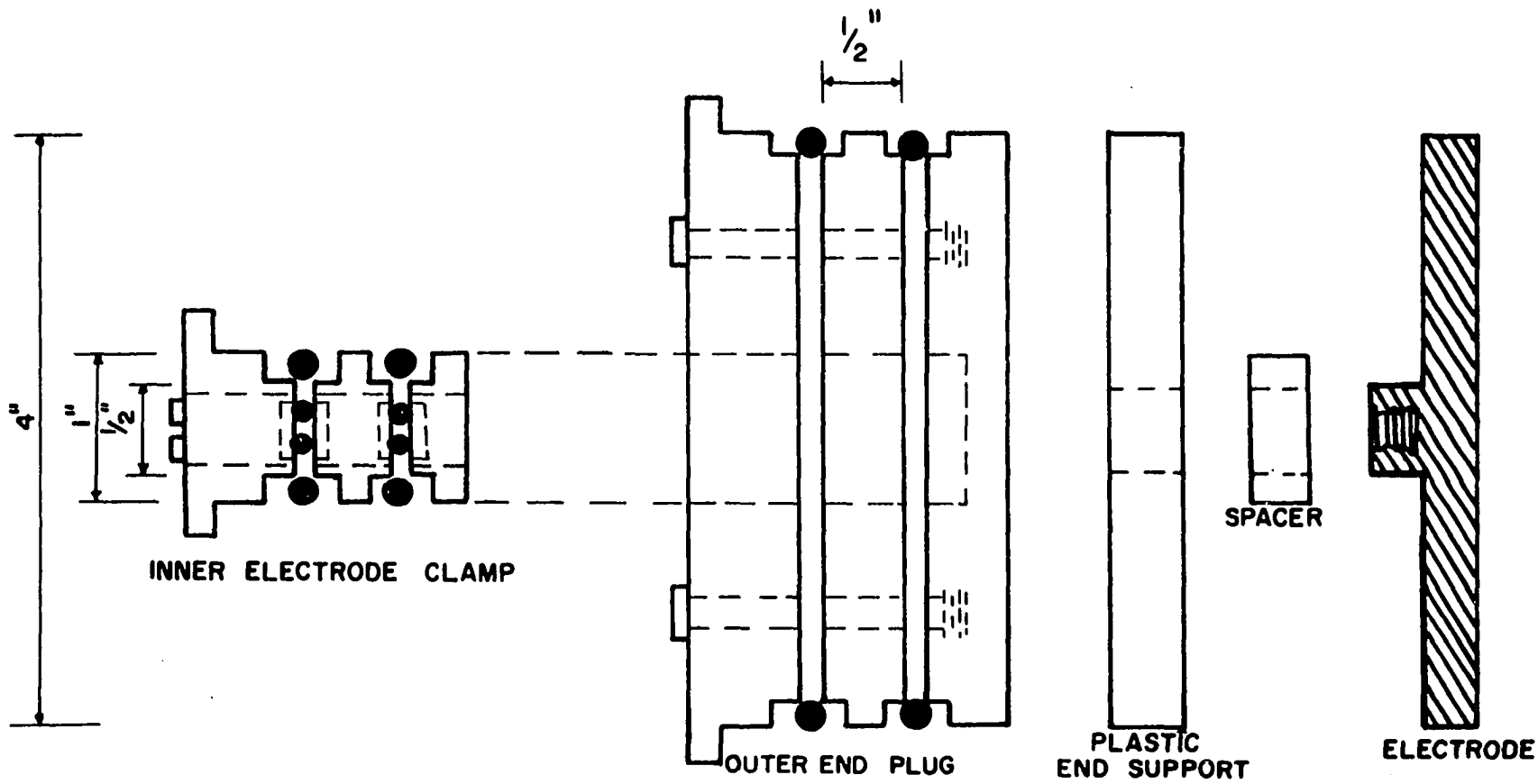
The test section was maintained at lowered pressures by means of vacuum forepumps connected to ports at either end of the tube. The tube pressure could be controlled over a nominal range of 200 to 5000 microns of mercury.

The near field probes were introduced into the media by means of coupling to a standard BNC UG492 A/U feedthrough connector. The probes were connected to shielded coaxial line from the connector to the detector. The connector was a sealed feedthrough capable of maintaining the desired pressure differentials.

A photograph of the test section is shown in Figure 3.

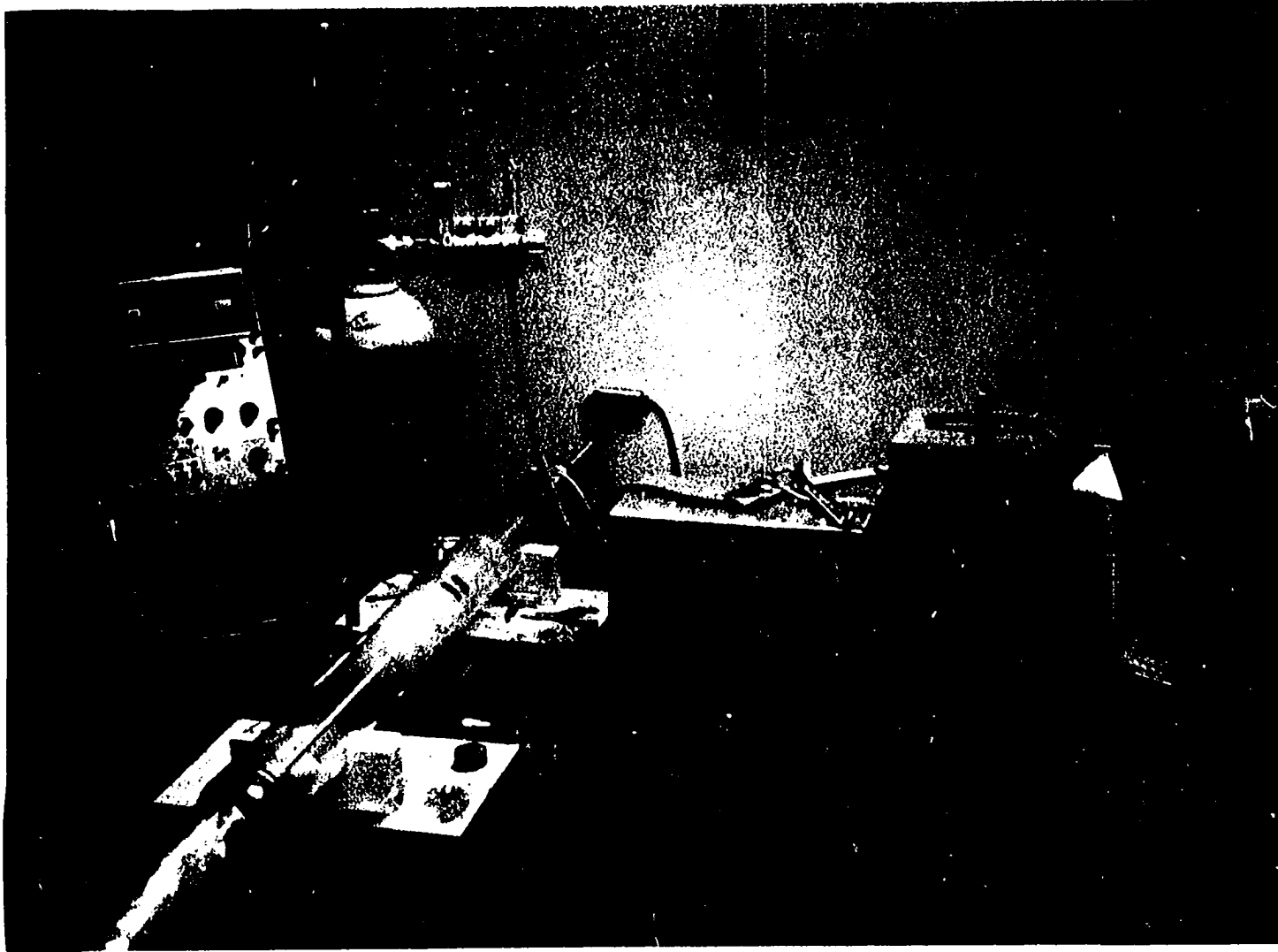
High Voltage Power Supply

The high voltage power supply system consisted of a number of fixed and variable voltage power supplies with a 100 milliam-



ELECTRODE SUPPORT ROD
 END PLUG CONFIGURATION

Figure 2



Photograph of Test Section
Figure 3

pere capability. In order to obtain the necessary voltage capability to satisfy the several possible experimental configurations, it was necessary to have a power supply with variable potential and current. Since no single supply of this capacity was available at the time of these experiments, a number of power supplies were connected in series to provide the desired levels of operation.

Three Lambda Model 25 power supplies rated at 275 to 325 volts and 100 milliamperes regulated output were used with three Lambda Model 71 power supplies rated at 0 to 500 volts and 100 milliamperes regulated output. Other supplies available for use included three 0-500 volt, 100 milliampere unregulated output power supplies built by the University of Oklahoma, School of Electrical Engineering. The total available voltage at 100 milliamperes was 3975 volts maximum.

This value of voltage was necessary, since the tube must be operated on a reasonable load line to provide stability of the plasma column. The power supplies were connected in series with each other and in series across the tube.

Vacuum System

The vacuum system consisted of two vacuum forepumps working at opposite ends to the test section. One of the pump assemblies was a W. H. Curtin and Co. 1/3 horsepower, 115 volt, 6.4 ampere, 60 cycle, 450-475 rpm motor with Wagner vacuum pump, while the other was a W. M. Welch vacuum pump driven by a capacitor-start induction-run 1/2 horsepower, 115 volt, 6.6 ampere, 375 rpm motor. The system

was found to provide sufficient volume capability to overcome the outgasing of the plastic tube and electrodes when operated at maximum current level.

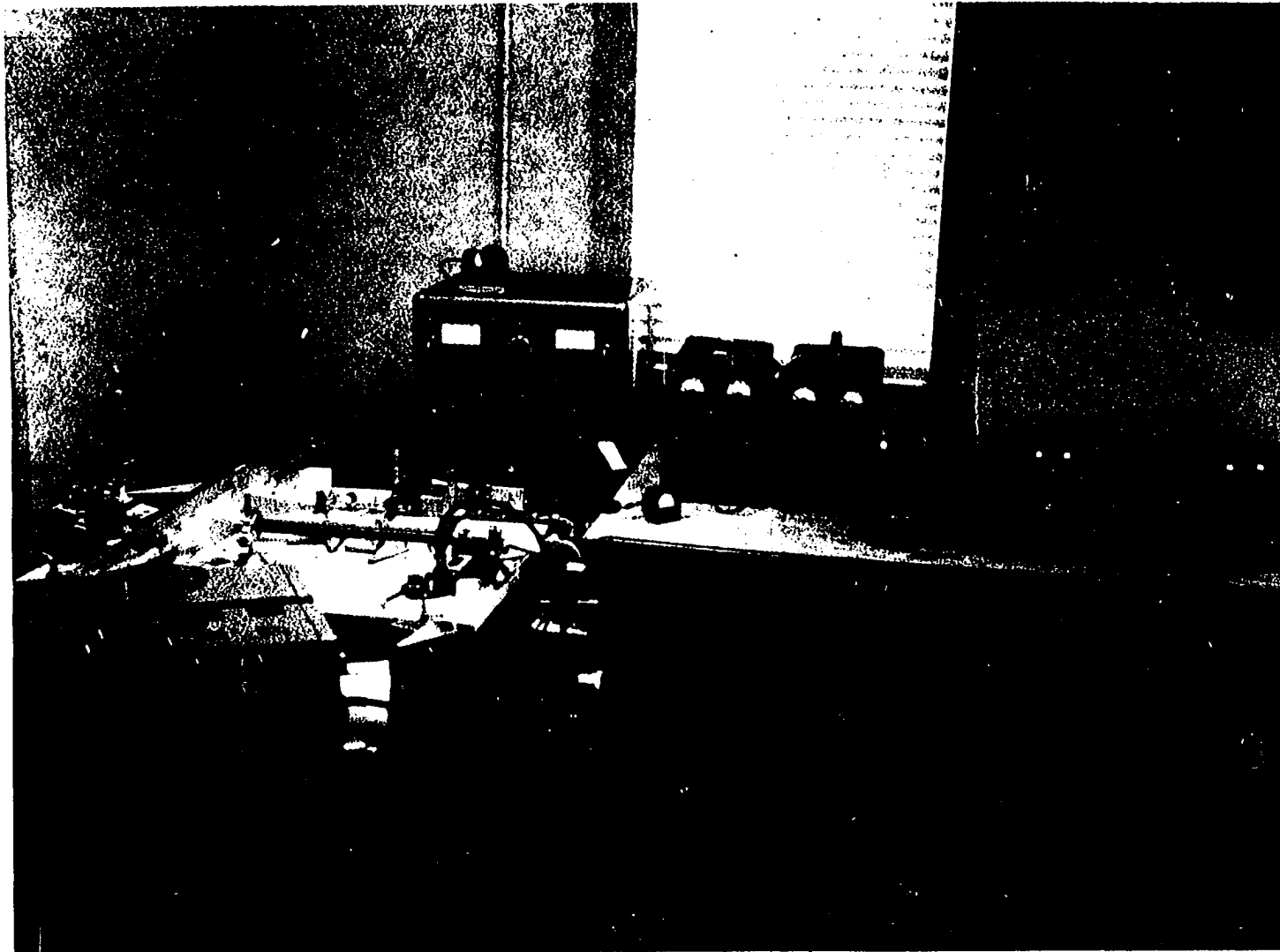
Measuring Instruments and Recording Devices

Pressure. The pressure was determined by use of a McLeod vacuum gauge operating directly in the test section. The range of pressures covered by this instrument is from 0 to 5000 microns. The usable range extends over 5 to 5000 microns. The pressure is read at each data point and recorded in the original data book.

Volt-ampere characteristic. The volt-ampere characteristic was measured by standard techniques using a Simpson Model 203 volt-ohm-milliammeter and a General Electric 0-100 milliamperes ammeter. The control of these parameters was supplied through power supply and the data was recorded in the data book.

Microwave Diagnostic Equipment

An X-band and K_a -band interferometer were used to help determine the plasma characteristics. The microwave bridge circuit is constructed of commercially available parts in which the unknown quantity is placed in one arm of the bridge. In the case of the interferometer the unknown is the plasma. The test section is placed between two sectoral horns and the phase shift of a known signal is related to the electron density.



Microwave Diagnostic Equipment
Figure 4

CHAPTER IV

PROCEDURE

The initial portion of the experimental program concerned itself solely with the determination of the plasma parameters; the manner in which they could be varied and the degree to which they could be controlled; and the testing of the probes that were to be utilized in the program. The final phase of the program consisted of the measurements under plasma conditions. Since the experimental portion falls naturally in these divisions, the procedure for each is reported as a separate subsection.

Plasma Tube Parameters

The tube parameters were measured while operating the positive column over a considerable range. The independent parameter for these measurements was the pressure in the test section, since the least amount of control could be exercised over this variable. The tube was connected to the vacuum pumps and vacuum measuring apparatus and the vacuum system turned on. The time required to obtain operational pressures of approximately 250 microns varied from 15 minutes to a half-hour, depending on the conditions in the tube prior to starting. After reaching the desired pressure level, high voltage was applied to the tube. Care was taken to assure

operation on a proper load line for protection of the tube against arcing conditions and to prevent the extinguishing of the positive column due to instabilities. The pressure was maintained at a constant value for each set of measurements.

While the pressure was held at a constant value, the input voltage to the tube was varied over a range sufficient to obtain the volt-ampere characteristic within the normal glow discharge region. Since the tube may be likened to a cold-cathode gas diode, the volt-ampere characteristic was expected to show a Townsend region, normal glow region and an abnormal glow. A typical characteristic is shown in Figure 5.

The measurements made, as described above, were then continued at two different pressures. These pressures were 400 and 1000 microns of mercury, respectively. The data taken over these trial runs is presented in Figures 27, 28, 29 and 30, Appendix A.

When the measurements were completed for the electrodes used above, a different set of electrodes was installed and similar measurements recorded. Electrodes of copper, aluminum and iron were used. The aluminum electrodes used were drilled to several patterns to ascertain which configuration was most suitable for the investigation pursued. A set of curves for these measurements is given in Figures 27, 28, 29 and 30, Appendix A.

Probe Measurements

Preliminary measurements were made to ascertain if the interior and exterior probe readings were the same in the absence of the

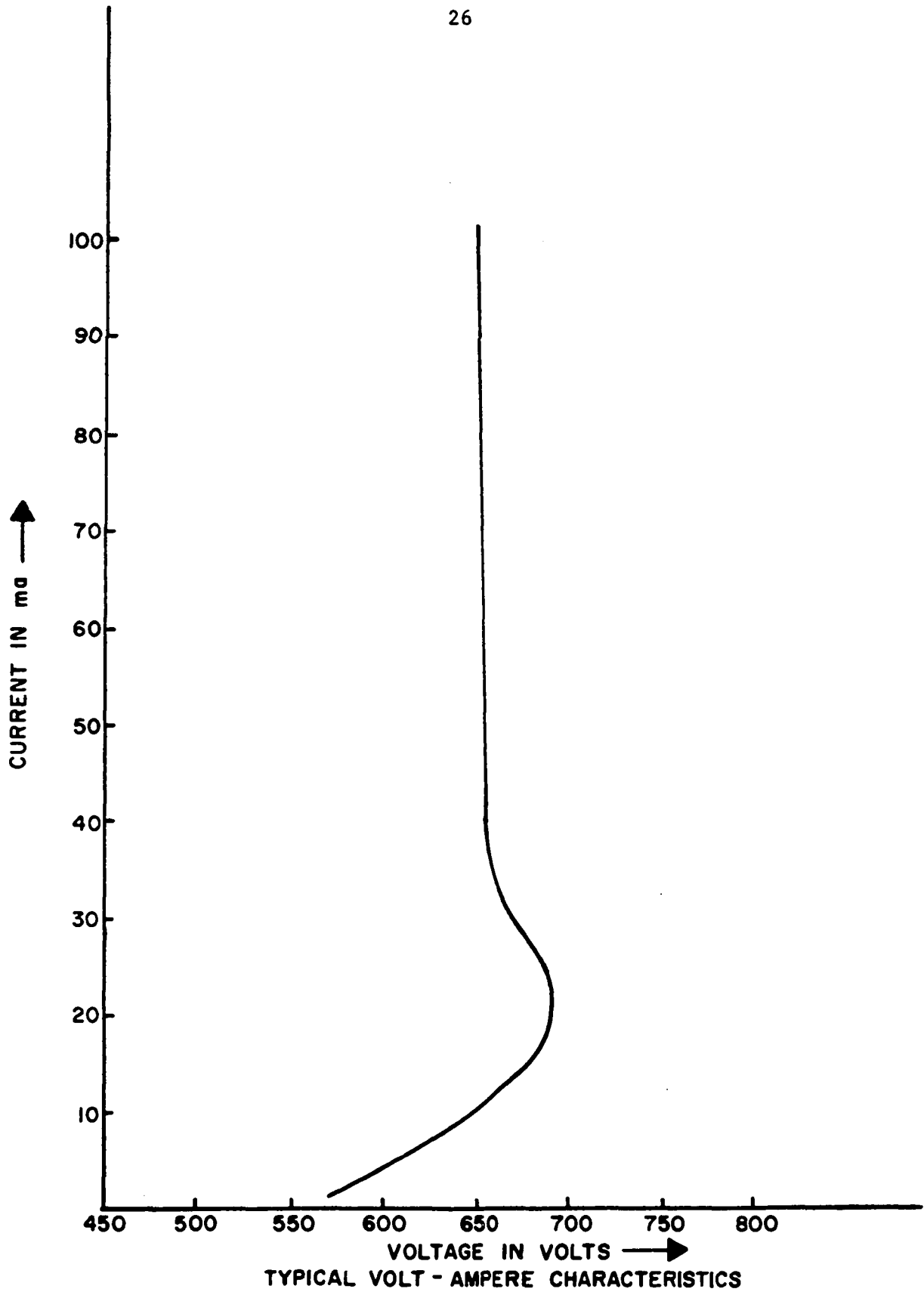


FIGURE 5

plasma. A check of the characteristics was made at several points over the frequency ranges that were to be expected. A relative response only was made, since the only requirement was that the two probes react in the same manner to the same applied signal.

Recurrence Measurements

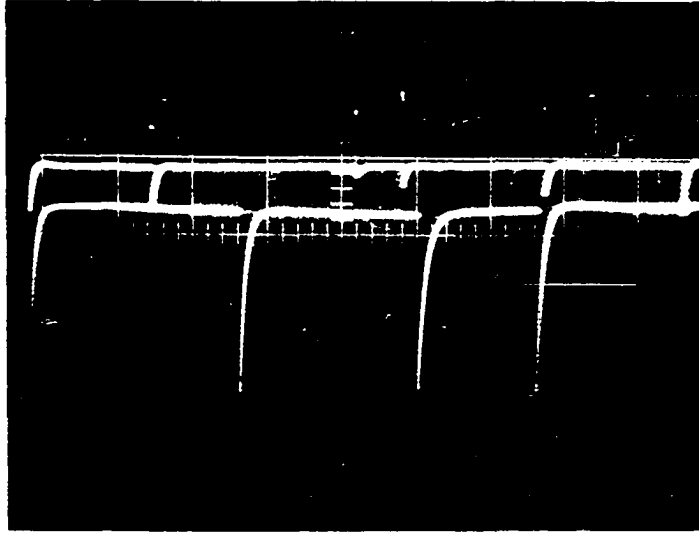
The frequency of occurrence of the electromagnetic waves detected from both the interior and exterior probes was to be determined as accurately as possible. With a known sweep time and shutter speed, an oscilloscope tracing was photographed and the number of events that had occurred was recorded. This technique allows the simultaneous recording of both waveforms. To provide a count in the quantity required for statistical sampling, a Hewlett-Packard Model 512 Electronic Counter was employed. The conditions of the tube were established and recorded. At a predetermined sampling rate (1 second or 10 seconds gate time) the outputs of the two probes were alternately read. This data was read and recorded in the original data book. This data appears in Tables 5 and 6 of Appendix C.

Electromagnetic Emission Characteristics

The characteristics of the electromagnetic waves emanating from the plasma were determined in two manners. The first was a sweeping of frequencies from 200 kilocycles per second to 900 megacycles per second and spot checking for characteristic emission at 9 kilomegacycles per second and 35 kilomegacycles per second. The output of the pickup was connected to a variety of receivers

including a BC-348-J Radio Receiver, a Hewlett-Packard Model 417A detector and an AN/APR-4 Microwave receiver. These units are each continuously tunable over a wide range of overlapping frequencies. For the purposes of measurement a particular plasma condition was established and maintained constant. The output of the pickup was scanned over the entire range of frequencies and characteristic frequencies or bands of frequencies were noted and recorded in the original data book.

The second method of examination was to display the output on a Tektronix Model 543 oscilloscope. In this manner, the wave shapes falling within the range of the oscilloscope could be examined in great detail. The output was displayed for several tube parameters and the data recorded with an oscilloscope camera Tektronix Model C-12 and entered in the original data book. The wave shapes were examined in detail for both rise and decay times, thus, a great many wave shapes were recorded. Typical oscilloscope tracings are shown in Figure 6.



T = 50 milliseconds/cm
Upper Trace A = .1 volts/cm
Lower Trace A = Arbitrary Amplitude

TYPICAL PROBE WAVESHAVE

Figure 6

CHAPTER V

THEORY

Introduction

As has been pointed out in previous chapters, the medium utilized in the experimental portion of this program has been that provided by a glow discharge. The observed phenomenon requires a definitive theoretical treatment of the glow discharge with particular attention to be given to the positive column and the cathode fall regions as they occur in normal glows. In addition, a quantitative statement pertaining to the manner in which induction fields are established by a moving charge is a necessity. In conjunction with the induction fields produced by an accelerating charge, several other possible mechanisms are considered from the physical standpoint and are included in Appendix B.

A hypothesis is presented to explain the phenomena observed experimentally. The basis of this hypothesis is placed on theoretical and experimental work performed by a great many researchers. The relationship of the observed phenomenon and fundamental processes in gaseous electronics is established and the significance of the experimental results is related to measurable characteristics in the normal glow discharge.

Theory of the Cathode Fall (7, 21, 31)

The cathode fall region of a glow discharge is found between the cathode and the negative glow region. The boundaries of the cathode dark space are well defined on both sides. In general, the Aston dark space and the cathode layer may be neglected when considering the theoretical development of the cathode fall or potential. Figure 7 shows the pertinent features of the glow discharge.

The three major regions of the glow discharge are the cathode dark space, cathode glow region and the positive column. The cathode dark space is characterized by the fact that no light is emitted. In general, the negative zones of the glow discharge follow the movement of the cathode, while the positive column adjusts itself to the particular situation. This is due to the beam characteristic of the negative regions and the swarm characteristics of the positive column. The emission of light from the negative regions follows Seeliger's rule in that the boundary is distributed according to the energy. Thus, in the cathode layer, the lower energy emissions take place nearest the cathode, while in the negative glow region, the high energy emissions take place nearest the cathode.

The theory of the cathode fall may be developed in the following manner:

Refer to Figure 7 and note the distance between the cathode and the boundary of the cathode glow region as d_c . The relation of the field and distance is given immediately below.

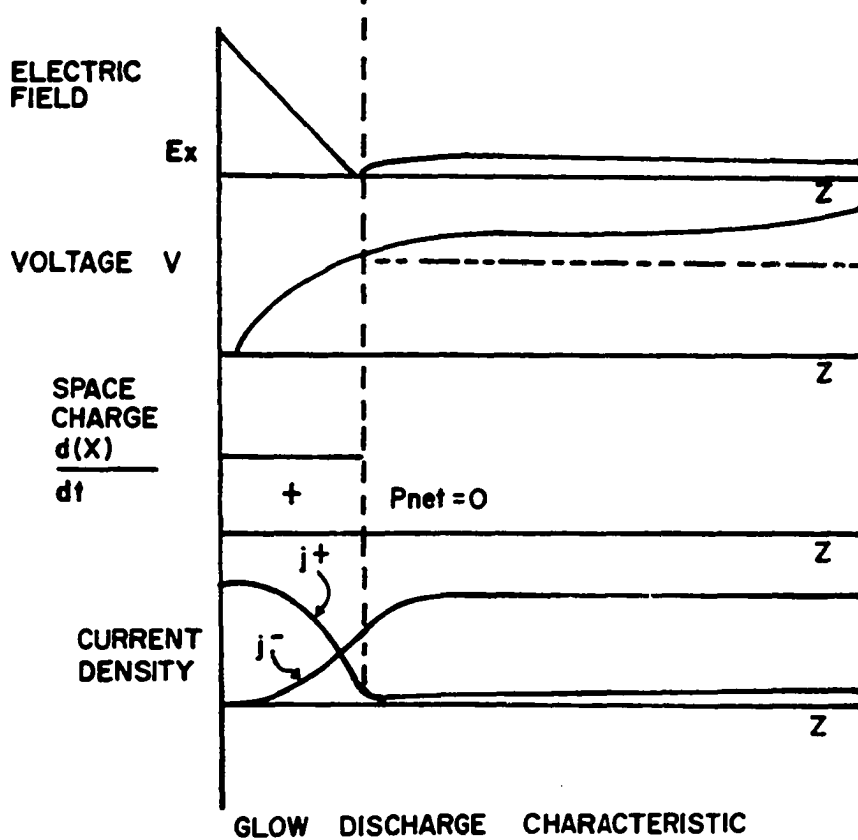
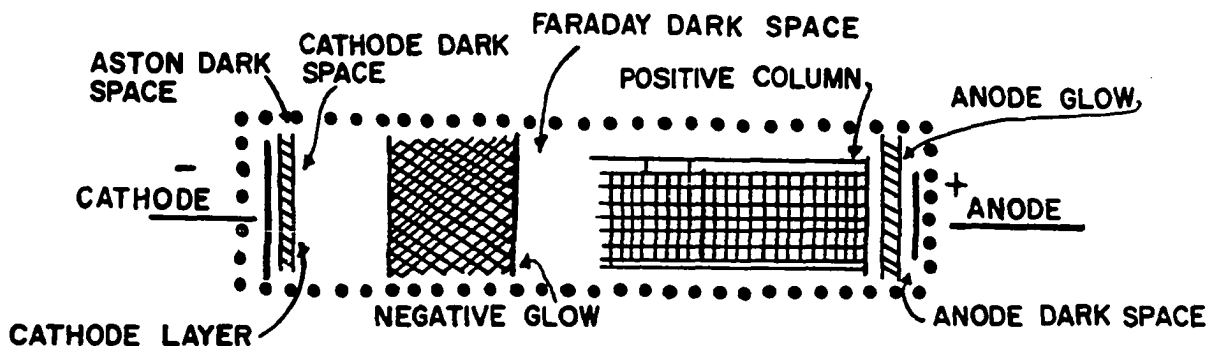


FIGURE 7

$$d_c E_c = 2V_c \quad \text{or} \quad E_c = 2V_c/d_c \quad (1)$$

let γ = number of secondary electrons/ion at the cathode

$$j_c = \text{total current} = j_c^+ + j_c^- = j_c^+ + \gamma j_c^+ = j_c^+(1+\gamma) \quad (2)$$

now using Poisson's equation

$$\frac{dE}{dx} = 4\pi\rho^+ \quad (3)$$

and the equation of continuity

$$j_c^+ = \rho^+ v^+ \quad (4)$$

$$\text{thus, } \frac{dE}{dx} = 4\pi \frac{j_c^+}{v^+} = \frac{4\pi j}{(1+\gamma)^+} \frac{1}{E} \quad (5)$$

$$\frac{E^2}{2} = \frac{4\pi j d}{(1+\gamma)} \quad \text{and} \quad j = \frac{E^2 \mu^+}{8\pi d} (1+\gamma) \quad (6)$$

and finally

$$j = \frac{v_c^{\mu^+}}{2\pi d^3} (1+\gamma) \quad (7)$$

Introducing the first ionization coefficient

$$\int_0^d \alpha dz = \ln(1+1/\gamma) \quad (8)$$

thus the number of positive ions

$$(e^{\int \alpha dz} - 1) = 1 \quad (9)$$

leading to the semi-empirical equations

$$\frac{\alpha}{p} = A \exp\left[-B/(X/D)\right] \quad (10)$$

$$\frac{E}{E_c} = 1 - \frac{Z}{d} \quad (11)$$

which have a solution of the form

$$\frac{(C_1 V_c)^{1/3}}{(C_2 j)^{2/3}} \text{ I.L. } (C_1 V_c \cdot C_2 j)^{1/3} = 1 \quad \text{where } C_1 = f(A, B, \gamma) \quad (12)$$

$$C_2 = f(A, B, \gamma, \mu^+)$$

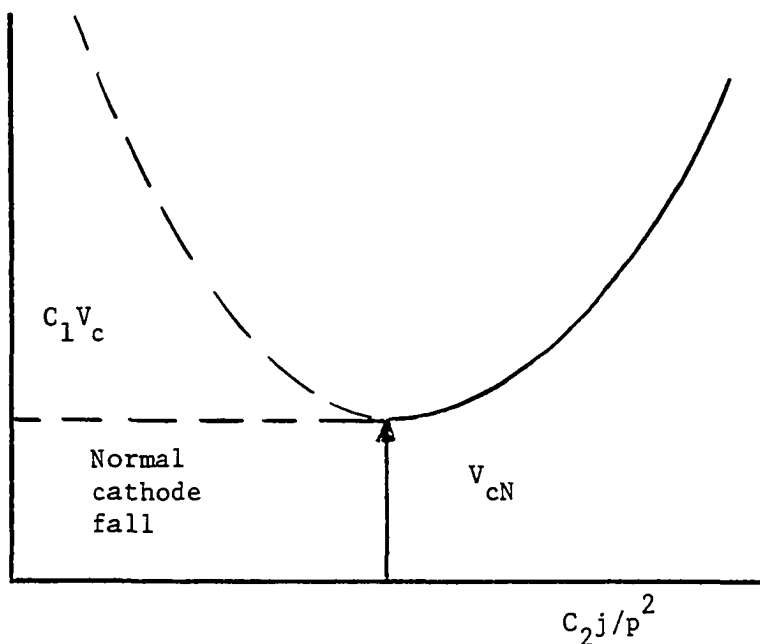


Figure 8

and I. L. = Integral Log.

By use of the similarity rules

$$\frac{j}{p} = \frac{V_c^2 (\mu^+ p)}{(pd)^{3/2}} (1+\nu) \quad (13)$$

The average number of ion pairs along a distance d is $\alpha d = \frac{V_c}{\eta}$

$$\text{and } \alpha dx = \ln\left(1 + \frac{1}{\gamma}\right) \text{ so that } V_c = \eta \ln\left(1 + \frac{1}{\gamma}\right) \quad (14)$$

where $\eta = E/d$ volts/ion pair or the number of volts an electron must fall through to produce an ion pair.

Theory of the Positive Column of the Normal
Glow Discharge (7, 21, 31)

The positive column of the normal glow discharge is completely independent of the other regions of the discharge when stable operating conditions have been achieved. The column itself has very little mechanical rigidity and will assume a form dictated by either

the confining boundaries of the vessel or the fields in which it operates or both. The positive column is characterized by a non-uniform radial and longitudinal current density, consequently, more visible energy is emitted from the center of the column than from the region near the wall or the regions toward the ends (particularly the more negative end) of the column. The current in the column is carried primarily by electrons, while positive ions compensate to allow a net charge imbalance of zero. This region is generally termed a plasma, a term coined by Langmuir (21) in 1929, to describe the conditions of a media with equal numbers of positive and negative charges. This region has further been termed the "fourth" state of matter, since the charges themselves are not individually neutralized but rather the overall column has a zero net concentration of charge.

The development of a complete theory of the positive column or plasma region of the glow discharge must include such physical aspects as ambipolar diffusion, radial field influence, charge density on the wall and the distribution of the charge density axially along the tube. The particular tube under investigation is a cylindrical tube, thus the theory will be developed for the case of cylindrical symmetry. The assumptions made are that only single collisions occur, no recombination within the column, no cumulative processes take place in the production of excited or metastable states, and that charges are neutralized at the wall. Included in the development is the electron temperature, the

radial electric field components and the density of particles in the column.

The number of charges lost from the center toward the wall in an element dr can be found by differentiation as:

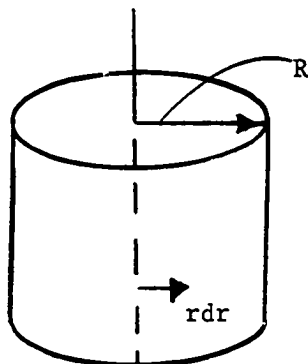


Figure 9

$$\text{loss in element } dr = -2\pi r D_a \left. \frac{dN}{dr} \right|_r - \left[1 - 2\pi(r+dr) \right] D_a \left. \frac{dN}{dr} \right|_{r+dr} \quad (15)$$

where D_a = ambipolar diffusion coefficient

$$\text{while the net gain} = \nu N 2\pi r dr \quad (\text{single electron collisions assumed}) \quad (16)$$

where ν = ionization rate/electron

Which leads to the differential equation

$$\frac{d^2 N}{dr^2} + \frac{1}{r} \frac{dN}{dr} + \frac{N}{D_a} = 0 \quad (17)$$

The differential equation above is Bessel's equation for zero order which has a solution:

$$\frac{Nr}{N_0} = J_0 \left(\sqrt{\frac{\nu}{D_a}} r \right) \quad (18)$$

The argument of the zero order Bessel function may be evaluated by recalling the boundary condition of zero net charge at the walls of the tube. This boundary condition is satisfied by taking the first zero of the Bessel function, thus,

$$2.405 = \sqrt{\frac{\nu}{D_a}} R \quad (19)$$

The justification of taking the zero at the wall is ample if the assumption of a small negative space charge at the wall is accepted. The negative space charge serves to turn slow electrons back into the plasma, while the fast electrons maintain equilibrium by replacing electrons that leak away to the walls. Neutralizing this negative space charge is a positive ion sheath that forms close to the wall. This sheath may be neglected if the ionic mean free path in the positive column is small compared to the radius of the tube. The radial distribution of charges is valid over a large range of tube pressures and electron temperatures, and is based on a Maxwellian velocity distribution function. It does not hold for large values of T_e/V_i , since few collisions would be observed, while for large values of pd the column contracts and degenerates to a spark discharge.

The ambipolar diffusion coefficient is given by:

$$D_a = \mu + \frac{kT_e}{C} \quad \text{where } \mu = \frac{e}{m} \frac{\lambda}{v} \quad (20)$$

while the ionization rate is found to be

$$\nu \propto p e^{-eV_i/kT_e} \quad (21)$$

hence $(cpR)^2 = F(T_e) \quad (22)$

Experimental results show that the electron temperature, T_e , is constant over the positive column in a normal glow discharge. The electron temperature relationship is as follows:

since

$$\nu = a p e^{-x} \quad \text{where } x = \frac{eV_i}{kT_e} \quad (23)$$

then

$$\frac{e^x}{\sqrt{x}} \propto p R^2 \quad \text{and} \quad D_a \propto T_e \propto \frac{1}{x} \quad (24)$$

therefore, D_p is constant for constant temperature. Consequently, as the walls are removed from the region of the glow the electron temperature decreases. This is because the losses at the wall are less, which requires fewer charges to be produced. The values of $N(r)$ and $T_e(pR)$ are known from experiment and the theoretical values show a good agreement over the valid range.

The radial field theory at present seems to be in doubt due to lack of agreement with observed results near the walls. The true value is found to be somewhere between the theory which states

$$E_r \propto \tan \sqrt{\frac{\nu}{D}} r \quad (25)$$

and

$$E_r \propto f(\sin \sqrt{\frac{\nu}{D}} x) \quad (26)$$

This discrepancy is not germane to the topics under consideration in this dissertation and no attempt will be made to justify either claims.

The aspects of the positive column in normal glow discharges that are pertinent to the experimental observations are related to the striations that are known to occur. At the present time, there is very little known concerning the true cause of this anomaly. The striation has been termed a region of cold ionized gas which propagates either toward or away from the anode region. The velocity of these striations (or waves of ionization) is reported by Loeb (21) to be faster from negative to positive. The experimental investigations performed in conjunction with this dissertation have resulted in an analysis of the wave shape of the striations and qualitative information with respect to the frequency of occurrence, randomness and amplitude.

Theoretical Relationships of Radiation Fields
from Accelerated Charges (23, 26, 27)

It has been well established that an accelerated charge will undergo an energy change and thereby radiate power in the form of an electromagnetic wave. Since this phenomenon is the underlying one for most of the possible radiation effects investigated in this report, this section will set forth the general relations between the accelerated charge and the subsequent radiation.

The general case of a radiating charge is one where the retarded position is known as a function of the retarded time:

$$z'_{\alpha}(t') = \text{retarded position} \quad (27)$$

$$t' = \text{retarded time}$$

The retarded time t' is equal to the time at which a signal with

a propagation velocity "c" is emitted from a retarded position $z'_\alpha(t')$ and will in turn arrive at position z_α at time t. The fields set up by an accelerated charge for which the retarded position z'_α is known, may be derived in the following manner:

$$\text{Let } u_\alpha = \frac{\partial z'_\alpha}{\partial t'} = \text{retarded velocity} \quad (28)$$

$$\dot{u}_\alpha = \frac{\partial u'_\alpha}{\partial t'} = \frac{\partial^2 z'_\alpha}{\partial t'^2} = \text{retarded acceleration} \quad (29)$$

Both u_α and \dot{u}_α are known by virtue of the defined knowledge of z'_α and t' . These terms may therefore be expressed in vector notation as follows:

$$-\bar{u} = \frac{d\bar{r}}{dt'} \quad (30)$$

$$-\dot{\bar{u}} = \frac{d^2\bar{r}}{dt'^2} \quad (31)$$

where \bar{r} = radius vector from the retarded position z'_α to the field point.

Since the retarded values of position and time are being used, it is necessary to express the potentials in the forms obtained by Liénard and Wiechert.

$$\varphi(z_\alpha, t) = \frac{e}{4\pi\epsilon_0 s} \quad (32)$$

$$\bar{A}(z_\alpha, t) = \frac{e}{4\pi\epsilon_0 c^2} \quad (33)$$

where e = charge in coulombs

ϵ_0 = permittivity of free space

c = velocity of propagation in meters per second

$$s = r - \frac{\bar{u} \cdot \bar{r}}{c}$$

Note that s is a function of the field point and the retarded position.

From the usual Maxwell equations the field functions may be determined:

$$\vec{B} = \nabla \times \vec{A} \quad (34)$$

$$\vec{E} = -\nabla\phi - \frac{\partial \vec{A}}{\partial t} \quad (35)$$

where \vec{B} = magnetic field density

\vec{E} = electric field intensity

The partial derivatives are functions of z_α and t , hence, a transformation must be accomplished before the field vectors may be computed. The field and source points are connected by the retardation conditions as follows:

$$r \left[z_\alpha, z'_\alpha(t') \right] = f(z_\alpha, t') = c(t - t') \quad (36)$$

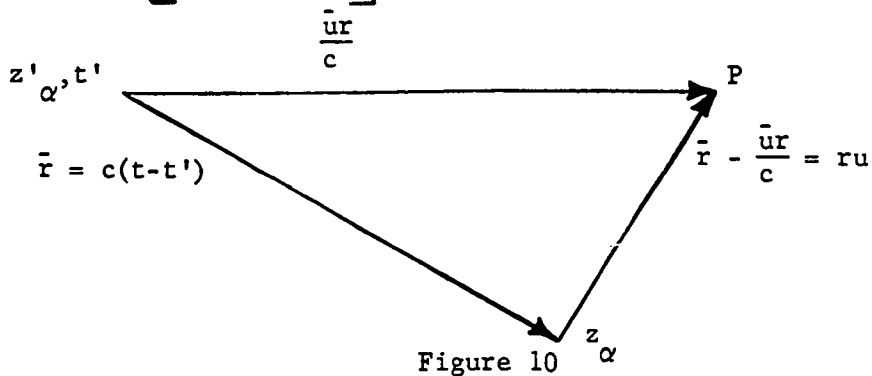


Figure 10

Field parameters for a moving charge:

z'_α, t' = retarded position

z_α = field position

P = virtual present position assuming constant velocity u .

Using these relations between z_α , t , and t' the transformations are determined as:

$$\left(\frac{\partial \bar{r}}{\partial t'}\right)_{z_\alpha} = \frac{\bar{r} \cdot \bar{u}}{c} \quad (37)$$

$$\frac{\partial \bar{r}}{\partial t} = c \left(1 - \frac{\partial t'}{\partial t}\right) = \frac{\partial \bar{r}}{\partial t'} \frac{\partial t'}{\partial t} = - \frac{\bar{r} \cdot \bar{u}}{c} \frac{\partial t'}{\partial t} \quad (38)$$

or

$$\frac{\partial t'}{\partial t} = \frac{1}{1 - \frac{\bar{r} \cdot \bar{u}}{c}} = \frac{r}{s} \quad (39)$$

hence

$$\frac{\partial}{\partial t} = \frac{r}{s} \quad (40)$$

using a parallel argument:

$$\nabla r = -c \nabla t' = \nabla r + \frac{\partial r}{\partial t'} \nabla t', \quad \nabla t' = \frac{\bar{r}}{r} - \frac{\bar{r} \cdot \bar{u}}{e} \nabla t' \quad (41)$$

therefore:

$$\nabla t' = - \frac{\bar{r}}{sc} \quad (42)$$

and in general $\nabla = \nabla_1 - \frac{r}{sc} \frac{\partial}{\partial t'}$ (43)

where ∇_1 , indicates derivatives with respect to the z_α coordinates.

Transforming equations (34) and (35) gives the potential functions as:

$$\begin{aligned} \frac{4\pi\epsilon}{e} \bar{E} &= \frac{1}{s^2} \nabla s - \frac{\partial}{\partial t} \frac{u}{sc^2} = \frac{1}{s^2} \nabla_1 s - \frac{\bar{r}}{cs^3} \frac{\partial s}{\partial t'} - \frac{r}{s^2 c^2} \bar{u} \\ &+ \frac{r\bar{u}}{c^2 c^3} \frac{\partial s}{\partial t'} \end{aligned} \quad (44)$$

using $\nabla s = \frac{\bar{r}}{r} - \frac{\bar{u}}{c}$, substituting and collecting terms:

$$\frac{4\pi\epsilon_0}{e} \bar{E} = \frac{1}{s^3} \left(\bar{r} - \frac{r\bar{u}}{c} \right) \left(1 - \frac{u^2}{c^2} \right) + \frac{1}{c^2 s^3} \left\{ \bar{r} \times \left[\left(\bar{r} - \frac{r\bar{u}}{c} \right) \right. \right. \quad (45)$$

$\left. \left. \times \bar{u} \right] \right\}$
similarly

$$\frac{4\pi\epsilon_0 c^2}{e} \bar{B} = \nabla \times \frac{\bar{u}}{s} = \frac{\bar{u} \times \bar{r}}{s^3} \left(1 - \frac{u^2}{c^2} \right) + \frac{1}{cs^3} \frac{\bar{r}}{r} \times \left\{ \bar{r} \times \left[\left(\bar{r} - \frac{r\bar{u}}{c} \right) \times \bar{u} \right] \right\} \quad (46)$$

thus;

$$\vec{B} = \frac{\vec{r} \times \vec{E}}{rc} \quad (47)$$

and the magnetic field vector, \vec{B} , is always perpendicular to the plane containing both \vec{E} and the retarded radius vector, \vec{r} .

The electric field vector, \vec{E} , is composed of two separate parts. The first term equation (44) shows variation as $\frac{1}{r^2}$, and is called the inductive field, implying that the detection is in the induction zone of the radiator. If $\vec{r}_\alpha = \vec{r} - \frac{r\vec{u}}{c}$ is defined as the position the charge would occupy at present if it had uniform velocity, then the induction field becomes:

$$\vec{E}_{\text{ind}} = \frac{e\vec{r}u}{4\pi\epsilon_0 s^3} \left(1 - \frac{u^2}{c^2} \right) \quad (48)$$

which may contribute to the net energy loss of the charge, but is not radiating in the sense that it does not contribute to the net energy flow over a surface at infinity.

The second term of (44) varies as $\frac{1}{r}$ and is termed the radiation field which does contribute to the net energy flux over a surface at infinity. This field is given by

$$\vec{E}_{\text{rad}} = \frac{e}{4\pi\epsilon_0 s^3} \frac{1}{c^2} \vec{r} \times (\vec{r} \times \ddot{\vec{u}}) \quad (49)$$

By similar deduction the magnetic field of (45) exhibits similar properties.

$$\vec{B}_{\text{rad}} = \frac{\vec{r} \times \vec{E}_{\text{rad}}}{rc} \quad (50)$$

Now Poynting's vector for the power flow is given by:

$$\vec{P} = \vec{E} \times \vec{H} = \vec{E}_{\text{rad}} \times \frac{\vec{B}_{\text{rad}}}{\mu} \quad (51)$$

$$\vec{P} = \frac{\vec{E}_{\text{rad}} \times (\vec{r} \times \vec{E}_{\text{rad}})}{\mu r c} \quad (52)$$

$$\vec{P} = \frac{1}{\mu r c} \left[|\vec{E}|^2 \vec{r} - \vec{E}(\vec{r} \cdot \vec{E}) \right]$$

$$\vec{E} = \frac{q}{4\pi\epsilon_0 c^2} \left((\vec{u} \cdot \vec{r}) \vec{r}_u - (\vec{r}_u \cdot \vec{r}) \vec{u} \right) \quad (53)$$

$$|\vec{E}| = \frac{q}{4\pi\epsilon_0 c^2} \left| (\dot{u} r \cos \theta) \vec{r} - (r_u r \cos \theta) \vec{u} \right| \quad (54)$$

$$\frac{\text{Power radiated}}{\text{Solid angle}} = \frac{dw}{dt}, \quad d\Omega = P \frac{dt}{dt'}, \quad \left[r^2 d\Omega \right] \quad (55)$$

$$P = \vec{E} \times \vec{H} = \frac{\vec{E} \times (\vec{r} \times \vec{E})}{\mu r c} \quad (56)$$

$$\text{where } \vec{E} = k_1 \left(\vec{r} \times (\vec{r}_u \times \vec{u}) \right) \quad (57)$$

$$\text{with } k_1 = \frac{q}{4\pi\epsilon_0 c^2} \quad (58)$$

$$P = k_2^2 \left\{ \left[\vec{r} \times (\vec{r}_u \times \vec{u}) \right] \times \left(\vec{r} \times \left[\vec{r} \times (\vec{r}_u \times \vec{u}) \right] \right) \right\} \quad (59)$$

$$\text{where } k_2 = \frac{k_1^2}{\mu r c}$$

$$\text{Let } \vec{A} = (\vec{r}_u \times \vec{u})$$

$$P = k_2^2 \left(\left[\vec{r} \times \vec{A} \right] \times \left[\vec{r} \times (\vec{r} \times \vec{A}) \right] \right)$$

$$= k_2^2 \left((\vec{r} \times \vec{A}) \times \left[(\vec{r} \cdot \vec{A}) \vec{r} - r^2 \vec{A} \right] \right)$$

$$= k_2^2 \left\{ \left(r^2 \vec{A} - (\vec{r} \cdot \vec{A}) \vec{r} \right) \times (\vec{r} \times \vec{A}) \right\} = k_2^2 \left[r^2 A^2 - (\vec{r} \cdot \vec{A})^2 \right] \vec{r}$$

$$+ \left[-r^2 (\vec{A} \cdot \vec{r}) + (\vec{r} \cdot \vec{A}) r^2 \right] \vec{A} = k_2^2 \left(r^2 A^2 - (\vec{r} \cdot \vec{A})^2 \right) \vec{r}$$

$$P = \frac{k_1^2}{\mu r c} \left(r^2 \left[\dot{u}^2 r_u^2 - (\vec{u} \cdot \vec{r}_u)^2 \right] - \left[\vec{r} \cdot (\vec{r}_u \times \vec{u}) \right]^2 \right) \vec{r} \quad (60)$$

$$\therefore \frac{dW(\theta)}{dt'} d\Omega = k_1^2 r \left\{ r^4 \left[\dot{u}^2 r_u^2 - (\vec{u} \cdot \vec{r}_u)^2 \right] - r^2 \left[\vec{r} \cdot (\vec{r}_u \times \vec{u}) \right]^2 \right\} \quad (61)$$

$$\frac{dt}{dt'}, d\Omega$$

$$\vec{\Psi} = \frac{dW(\theta)}{dt'} d\Omega$$

$$\begin{aligned} \bar{\psi} &= \frac{q^2 r^2}{16\pi \epsilon^2 s^3 c^4 \mu} \left\{ \bar{r} \left(r^2 \left[\dot{u}^2 r_u^2 - (\bar{u} \cdot \bar{r}_u)^2 \right] - \left[\bar{r} \cdot (\bar{r}_u x \bar{u}) \right]^2 \right) \right\} \frac{s}{r} d\Omega \\ \psi &= \frac{q^2 r}{\mu 16\pi \epsilon^2 s^5 c^5} \left\{ \bar{r}_o \left(r^2 \left[\dot{u}^2 r_u^2 - (\bar{u} \cdot \bar{r}_u)^2 \right] - \left[\bar{r} \cdot (\bar{r}_u x \bar{u}) \right]^2 \right) \right\} d\Omega \quad (62) \end{aligned}$$

where $\bar{r}_o =$ unit vector.

This may be rewritten as:

$$\bar{\psi} = \frac{q^2 r \left[\bar{r} x (\bar{r}_u x \bar{u}) \right]}{16\pi \epsilon^2 \mu s^5 c^5} d\Omega \quad (63)$$

To determine the total rate of radiation we may put this expression in a more convenient form and integrate over the solid angle.

$$- \frac{dU}{dt'} = \int \frac{k \left[\bar{r} x (\bar{r}_u x \bar{u}) \right]}{s^5} d\Omega \quad (64)$$

Assuming that \bar{u} is a polar axis and integrating the azimuthal section first we find a final integral of the form:

$$- \frac{dU}{dt'} = \frac{q^2}{6\pi \epsilon c^3} \left\{ \frac{\dot{u}^2 - (\bar{u} x \bar{u})^2 / c^2}{1 - u^2 / c^2} \right\} \quad (65)$$

for the usual case where $u \ll c$ this then reduces to the simpler expression:

$$- \frac{dU}{dt'} = \frac{q^2 \dot{u}^2}{6\pi \epsilon c^3} \quad (66)$$

Near Zone Effects (23, 26, 27)

The expressions determined in this chapter are meant to be applied at distances which are large compared to the wavelength of the radiation. Such systems may be extended and similar expressions derived for each type of energy transformation mechanism.

If the system under observation is such that measurements are to be made at distances of the order of one wavelength or less, then a different approach must be used.

Assuming dipole radiation with a system of dipole moment \vec{d} , it has been shown that the scalar potential will be:

$$\varphi = -\nabla \cdot \frac{\vec{d}}{r}$$

where r = distance to the field point

$$r \leq \lambda$$

$$\text{and } \vec{E} = \nabla(\nabla \cdot \frac{\vec{d}}{r}) - (\frac{\ddot{\vec{d}}}{c^2 r})$$

$$\vec{H} = \frac{1}{c} \nabla \times \frac{\dot{\vec{d}}}{r}$$

From the precepts of vector analysis:

$$\vec{E} = \nabla \times \nabla \times \frac{\vec{d}}{r}$$

Using the standard technique for determination of the power flow in this region:

$$\vec{P} = \vec{E} \times \vec{H}$$

it is noted that in order to determine signal power flow it is necessary to determine the Fourier components for the field:

$$\vec{H}_\omega = jk\vec{d}_\omega \times \nabla \frac{e^{jkr}}{r}$$

$$\vec{E}_\omega = k^2\vec{d}_\omega \frac{e^{jkr}}{r} + (\vec{d}_\omega \cdot \nabla)\nabla \frac{e^{jkr}}{r}$$

$$\vec{P}_\omega = \vec{E}_\omega \times \vec{H}_\omega$$

where $k = \frac{1}{c}$

In the general case stated previously

$$\vec{E} = \nabla \times (\nabla \times \frac{\vec{d}}{r})$$

$$\begin{aligned}
\mathbf{H} &= k \left(\nabla \times \frac{\bar{\mathbf{a}}}{r} \right) \\
\bar{\mathbf{P}} &= k \left[\nabla \times \left(\nabla \times \frac{\bar{\mathbf{a}}}{r} \right) \right] \times \left[\nabla \times \frac{\bar{\mathbf{a}}}{r} \right] \\
&= k \left[\left(\nabla \cdot \nabla \times \frac{\bar{\mathbf{a}}}{r} \right) \left(\nabla \times \frac{\bar{\mathbf{a}}}{r} \right) - \left(\nabla \cdot \nabla \times \frac{\bar{\mathbf{a}}}{r} \right) \left(\nabla \times \frac{\bar{\mathbf{a}}}{r} \right) \right]
\end{aligned}$$

therefore, the Poynting vector $\bar{\mathbf{P}}$ is identically zero since for any vector $\bar{\mathbf{A}}$:

$$\nabla \cdot \nabla \times \bar{\mathbf{A}} = 0 \quad (67)$$

This result shows that in the near zone of the antenna or source of radiation no power flow is detectable by an observer. Since there are, however, both electric and magnetic harmonic fields, induction in this zone is possible. A similar calculation for other radiation source mechanisms (quadrupole and multipole) gives similar results.

The Hypothesis

A thorough review of the available literature in the fields of plasma physics, plasma dynamics, gaseous electronics, gas discharge phenomena, gaseous plasmas, and fusion research has failed to reveal a uniformly acceptable theoretical or experimental explanation of some of the processes related to secondary effects. The results of the experimental program performed in conjunction with this dissertation allows a hypothesis to be presented which, under the conditions of the experiment, represents a partial explanation of some of the secondary processes.

An experimental investigation of the electromagnetic emanation from static plasmas resulted in a series of unexplained wave-shapes recorded both inside and outside the confining tube. The exterior waveforms exhibited the general appearance of relaxation phenomena and were found caused by an induced effect from the glow discharge. With the experimental results at hand and utilizing the wealth of experimentally proven theoretical analysis as a base, the basic premise of the hypothesis may be stated as follows:

Having reached equilibrium conditions, as dictated by such ambient parameters as pressure, current density, voltage gradients, electron temperatures, etc., a multitude of primary and secondary effects occur to maintain the self-sustained glow discharge. Primary electrons, those drawn from the cathode, are accelerated across the cathode fall region of the discharge. These electrons

are assumed to possess a Maxwellian velocity distribution function. Prior theoretical and experimental works have shown that only the more energetic electrons leave the cathode layer and cross the well defined dark space to the negative glow region. The electrons that have entered this region have progressed a sufficient distance from the cathode so that their energy has again reached a value where the collision cross-sections are large enough for an efficient level of ionization (21). Thus, the existing situation is that the electrons have succeeded in giving rise to a large number of positive ions in the negative glow region which has the effect of disturbing the equilibrium of the negative glow. These surplus positive ions have a velocity distribution that is essentially the same as the electrons which initially provided the ionization energy. These ions are now influenced by the electric field gradients and are linearly accelerated across the cathode dark space to the positive space charge region surrounding the cathode. When they enter this space charge region they are non-linearly decelerated by the interaction of the coulomb type forces.

From the above hypothesis, postulations may now be made concerning the various types of energy transfer and experimentally observable parameters that are caused by this mechanism. As the primary electrons enter the negative glow region, ionizing colli-

sions occur with the molecules of the gas as well as the recombination effects. The ionizing collisions give rise to positive ions, which have undergone a non-linear acceleration. This non-linear acceleration should give rise to both an induction field and a radiation field as described by equations (48) and (49). This imbalance of positive ions is then linearly accelerated across the cathode dark space toward the positive space charge region. Again an accelerated charge radiates and this result should be of the form of a constant field strength. When these ions enter the positive space charge region they are non-linearly decelerated, again giving up some of their energy through radiation. The preceding may be interpreted in terms of a waveshape in either the near or far field zones as electromagnetic waves. This interpretation is depicted in Figure 11 for clarity and is explained in the following steps:

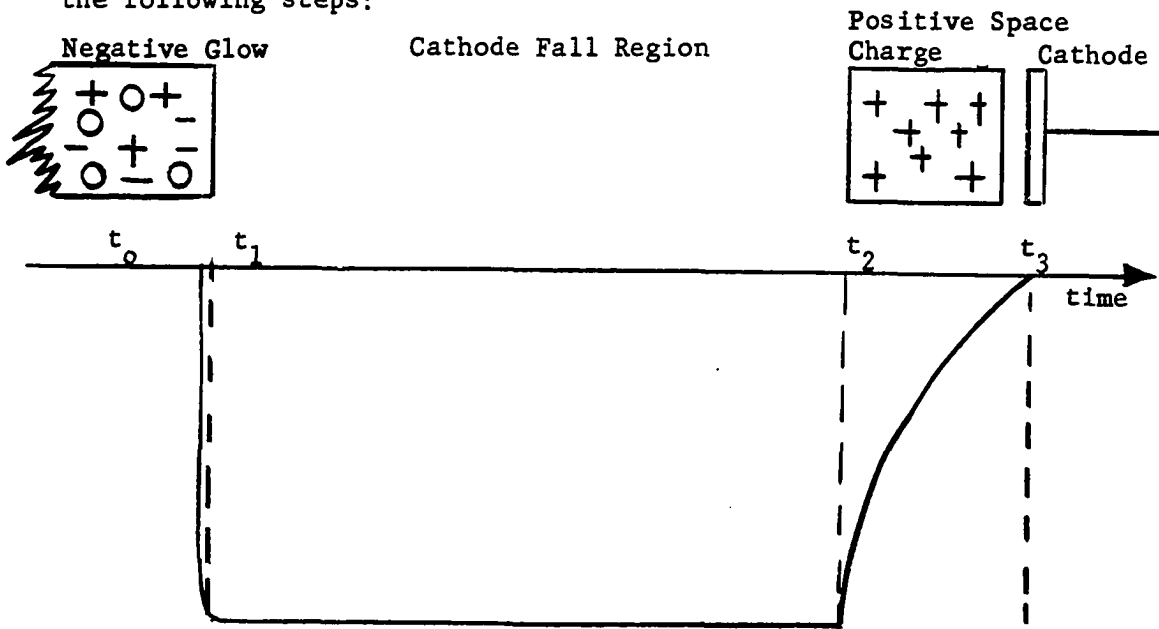


Figure 11

1. The initial rise in the relative amplitude between t_0 and t_1 may be attributed to the non-linear acceleration given to the positive ions through the ionizing collision of the primary electrons at the negative glow. This rise time should be relatively insensitive to the density of either the gas molecules or charged particles as well as the type of gas used in the discharge.
2. The constant relative amplitude occurring between t_1 and t_2 is a result of a charge undergoing a constant acceleration in the cathode dark space. As equation (48) shows, a charge undergoing a constant acceleration will give rise to a constant radiation and induction field. The duration of time (or distance) of this constant field strength should be a function of the relative mass of the particle being accelerated as well as field variations in the cathode dark space.
3. The decay of the relative amplitude, as shown in Figure 11 between t_2 and t_3 , is postulated to be due to coulombic force interaction between the positive space charge and the positive charges entering from the cathode dark space. This decay time should be a function of the density of the positive space charge until it is fully established. At the time this space charge is fully established around the cathode the decay time should reach its shortest time and remain at this value, independent of the mass of the positive ions.

These steps indicate the time-relative amplitude effect that is hypothesized. As a result of this hypothesis, postulation may now be made concerning the manner in which this interaction becomes a time recurring event. The postulation may be characterized in the following manner:

The primary electrons which enter the negative glow region were previously assumed to have a Maxwellian velocity distribution. The efficiency of ionization, as has been pointed out previously, is greatest for electrons around the average and most probable velocity distribution. The manner in which the event takes place may be assumed to occur qualitatively by dividing the primary electrons into differential elements, dz , as shown in Figure 12.

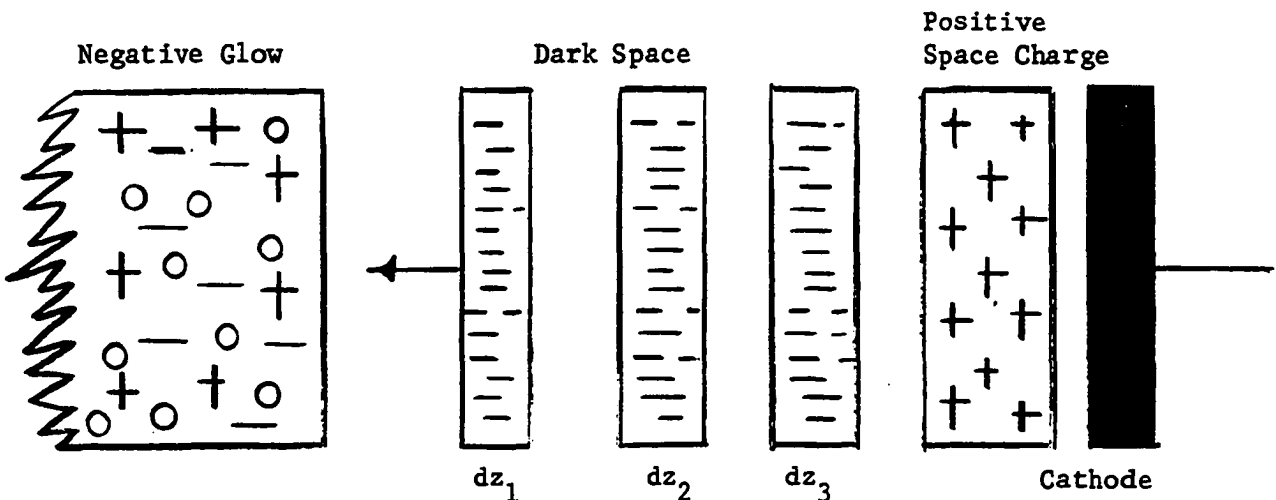


Figure 12

The differential element dz_1 may be considered to be the one giving rise to the waveshape just described. The energy removed from this element dz_1 in causing ionization leaves this element at an energy or temperature substantially lower than that of the electrons of the positive column. This cold "swarm" of electrons leaves the negative glow region and is accelerated to some extent through the Faraday dark space. This gain of energy still leaves these electrons at a lower relative energy than the positive column, thus, causing this region to appear dark as it progresses toward the anode. These cold "waves" of ionized gas have been termed striations and are clearly visible in the positive column of the gas discharge.

While this has occurred in the negative glow and Faraday dark space, the positive ions generated by dz_1 are being accelerated toward the cathode. The next element of electrons dz_2 now enters the negative glow region and, instead of the situation experienced by dz_1 , this element sees a surplus of positive ions. This swarm, dz_2 , thus loses the bulk of electrons through recombination and shuts off the supply of positive ions and electrons. The next element dz_3 sees a situation similar to that found by dz_1 and the sequence of events repeats.

The positive ions moving toward the cathode are not effected by the electrons from the cathode for at least two reasons. First, the energy of these electrons is higher than when they enter the negative glow region which lowers their ionization efficiency.

Second, the positive ions and electrons must undergo two-body recombination. The collision cross-section for two-body recombination is quite low (21), hence, the positive ions go on toward the cathode to give up their energy in either the positive space charge region or the cathode. This gives rise to a series of positive ion "waves" progressing toward the cathode in the same manner that the cold ionized gas "waves" are progressing toward the anode.

In the limit as dz goes to zero and the electrons form essentially a beam, it can be seen that current pulsations should occur due to the absorption of energy in the negative glow region. The recurrence of these positive and negative pulsations should be of either the same value, or if different, have a high correlation coefficient. It is highly probable that the recurrence rates will be different, since the electrons that cause the positive ion waves may themselves be recombined as they progress through the negative glow region. Thus, it should be expected that the positive ion waves would have a higher survival probability, hence, a higher repetition rate. The fact that a current pulse is postulated to occur is significant from the standpoint of explaining the occurrence of striations in glow discharge tubes. From this hypothesis, it is seen that the repetition rates for the negatively traveling positive ion swarm should be higher than that of the positively traveling electron swarm. This is contrary to statements made from measurements using phototubes to observe the striations (21).

The hypothesis is given qualitatively in the steps below:

1. Primary electrons from the cathode enter the negative glow region and suffer ionizing collisions with the neutral gas molecules.
2. The resulting positive ions, having been non-linearly accelerated, give rise to an induction field.
3. These ions are linearly accelerated across the cathode dark space, generating a steady field.
4. At the positive space charge region, the positive ions give up their energy with a non-linear deceleration causing the field to change toward zero.
5. The more energetic positive ions continue to the cathode giving up the remainder of their energy in the formation of secondary electrons.
6. The movement of the electrons caused by this process could be instrumental in the evolution of striations.

The hypothesis, as presented above, obeys the physical boundary conditions within the gaseous discharge and can be used to give a possible explanation to the occurrence of striations, to the energy lost through radiation and to the generation of some of the secondary effects. Mathematically, the hypothesis may be characterized as follows:

Assume that charges of a single sign are produced at the cathode surface. The current density, as given by equation (7) is

$$j = j_c^+ + j_c^- = j_c^+ + \gamma j_c^+ = (1+\gamma) j_c^+ = \frac{v_c^2 +}{2\pi d^3} (1+\gamma) \quad (7)$$

which corresponds to an initial charge density n_0 .

The charge density at any point d in the discharge is found by assuming that α ion pairs/cm are formed,

hence

$$dn = \alpha n_0 dx \quad (68)$$

and

$$\frac{n_d}{n_0} = e^{\alpha d} \quad (69)$$

The charges which fall on the negative glow region give rise to an induced field given as

$$\bar{E}_{ng} = E_{Tind} (1 - e^{-\xi t}) \quad (70)$$

where E_{Tind} = maximum value of the induced field

ξ = an empirical coefficient related to the density of molecules in the negative glow determined experimentally.

The positive ions caused by the ionizing collisions are linearly accelerated across the cathode dark space, causing a constant value induction field to appear

which is given by

$$E_{ind/ion} = \frac{e\bar{r}u}{4\pi\epsilon_0 s^3} \left(1 - \frac{u^2}{c^2} \right) \quad (48)$$

$$\text{hence } E_{Tind} = \frac{n_i e\bar{r}u}{4\pi\epsilon_0 s^3} \left(1 - \frac{u^2}{c^2} \right) \quad (71)$$

is the total field.

$$\text{where } s = r - \frac{\bar{u} \cdot \bar{r}}{c}$$

u = velocity of the positive ion

r = distance from source to field point.

When the accelerated positive ions intercept the positive space charge, the coulomb force interaction causes a non-linear deceleration, which has a field

$$\bar{E}_{sp} = \bar{E}_{T_{ind}} e^{-\psi t} \quad (72)$$

associated with it.

where ψ = an empirical coefficient related to the effective density of the positive space charge and is experimentally determined.

The total wave form of Figure 11 is of the following form:

$$\bar{E}_{ng} = \frac{n_i e \bar{r} u}{4\pi \epsilon_0 s^3} \left(1 - \frac{u^2}{c^2} \right) \left(1 - e^{-\xi t} \right) \quad t_0 \leq t \leq t_1 \quad (73)$$

$$\bar{E}_{T_{ind}} = \frac{n_i e \bar{r} u}{4\pi \epsilon_0 s^3} \left(1 - \frac{u^2}{c^2} \right) \quad t_1 \leq t \leq t_2 \quad (74)$$

$$\bar{E}_{sp} = \frac{n_i e \bar{r} u}{4\pi \epsilon_0 s^3} \left(1 - \frac{u^2}{c^2} \right) e^{-\psi t} \quad t_2 \leq t \leq t_3 \quad (75)$$

The relationships that have been developed allow a qualitative and/or quantitative interpretation of the following properties or processes that occur in ionized gases:

1. Determination of the effective density of positive ions in the space charge region.
2. Qualitative information concerning the loss of energy through radiation in the VHF frequency range.

3. A possible explanation of striations in glow discharges.
4. Knowledge concerning the effective distance between the positive space charge region and the negative glow.
5. An insight into secondary processes is possible through evaluation of the exponential terms, since these values are related to the rate of production and annihilation of positive ions.

CHAPTER VI

RESULTS

General Comments on Observed Waveforms

Electromagnetic probes were placed at various positions around the tube in an effort to determine the emission from the discharge as a function of frequency. Prior work in this field led to the anticipation of a noise spectrum emanating from the discharge. This noise spectrum was observed in the radiation field of the discharge by a variety of methods as outlined in Chapters III and IV. No characteristic emission was found to occur in the far field other than the noise spectrum which was easily attributed to be due to the sparking at the cathode.

While observing the characteristics of the plasma with the X-band interferometer, an unexplainable wave was found on the crystal-detector output. A spike of energy was found to appear that was aperiodic and of an indeterminate form. The cause was initially felt to lie in the microwave and wire circuitry or through false triggering of the oscilloscope. The spike was next found to occur in the output of a simple passive X-band horn and detector. The relative magnitude of this spike was determined to be two orders of magnitude

greater than the amplitude of the modulation wave on the X-band carrier of the interferometer and gave nearly one-tenth volt output from the passive horn. The wave shape in relation with the modulated X-band carrier is shown in Figure 13.

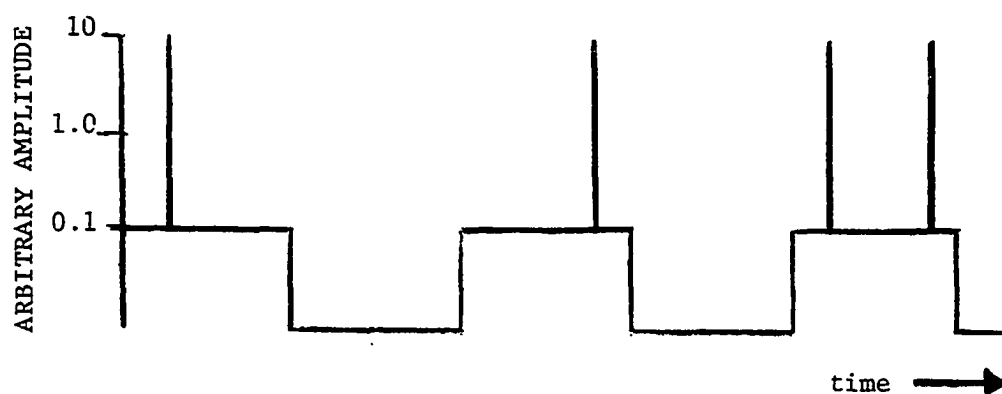


Figure 13

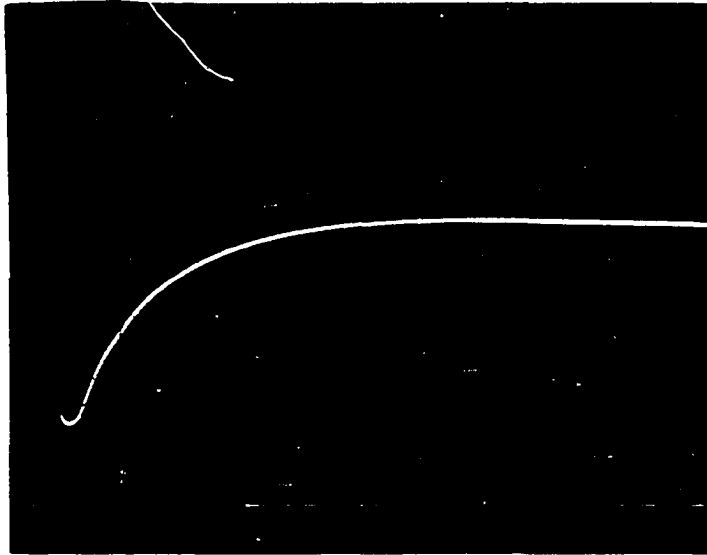
Further investigation revealed that this voltage spike was not a function of faulty microwave or wire circuitry or of the oscilloscope. In addition, it appeared that so long as the microwave horn was "looking" at the glow discharge at a relatively close distance (not greater than six inches) that this spike was independent of the geometry. At this point it was decided to perform a thorough experimental analysis of the anomaly. To this end the following steps were taken:

1. An electromagnetic pickup was located in the center of the positive column.
2. A Langmuir type probe was installed at the wall 90° from the electromagnetic probe.
3. An electromagnetic pickup with electrical characteristics identical to the one located inside was placed outside the tube directly opposite the interior probe.

The tube was thus instrumented to detect waves or pulses at the center of the discharge, at the wall and outside, for both near and far field measurements. The experimental procedure outlined in Chapter III was then followed. The resulting wave-shapes that were obtained are depicted in Figures 14 and 15. The time and relative amplitude scale of both are given in this figure so that a direct comparison may be made.

Interior Probe Waveform

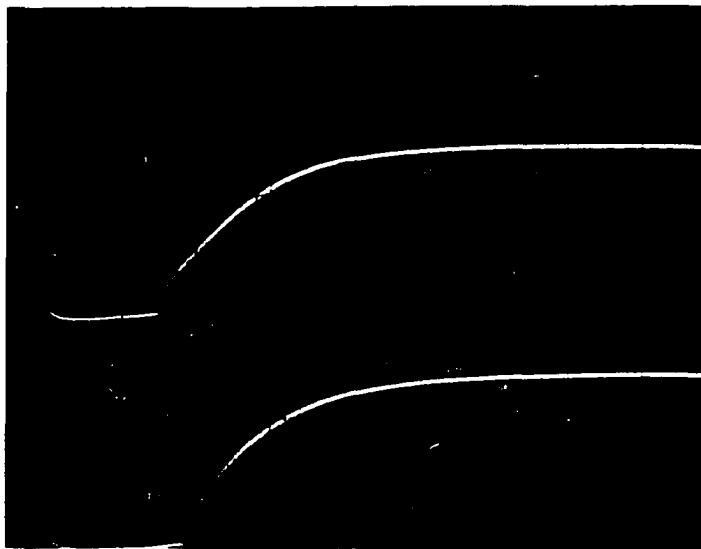
The waveform found in the positive column of the discharge is shown in Figure 14. An expanded time scale oscilloscope tracing of the same waveshape for analysis purposes is shown in Figure 16. From this tracing it can be seen that the time for the wave to reach maximum value is 2.2 microseconds and that the time required to decay to 63.2% of its maximum value is 250 microseconds. The rise and decay times of these voltage waveforms were found to be nearly independent of the tube current after a certain minimum level was attained. The minimum level of tube current was found to be a function of the pressure in the



T = 50 microseconds/cm
A = Arbitrary

Interior Probe Waveshape

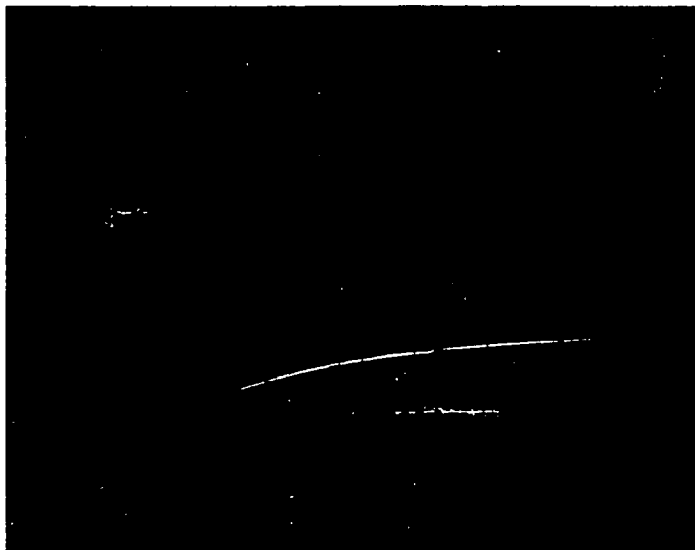
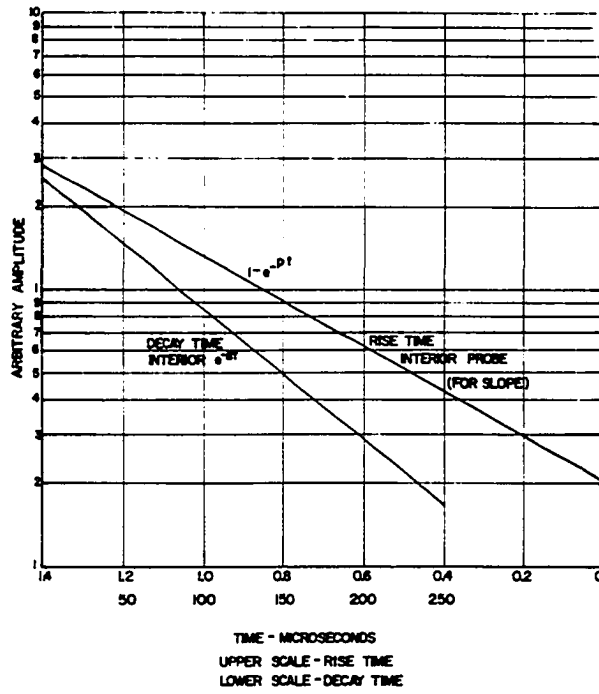
Figure 14



T = 2 microseconds/cm

Exterior Probe Waveshape

Figure 15



Upper Trace $T = 0.5$ microseconds/cm
 Lower Trace $T = 50$ microseconds/cm

Amplitude as a Function of Time for Interior Probe

Figure 16

tube. For the two pressures utilized in the experimental work, 400 and 1000 microns of mercury, the transition currents were found to be 14 and 37 milliamperes, respectively. The source of these waveforms was attributed to the striations traveling in the positive column. The relative amplitude of these voltage waveforms was found to be a function of the tube current up to the transition current at which point the amplitude attained its maximum value of 180 volts (with air as the gas in the tube). Fowler (13) originally suggested that these waveforms may be attributed to the passage of striations down the tube. He further indicated that an amplitude level of the value of the cathode fall should be found. This value of cathode fall for air is approximately 180 volts depending on exact nature of the conditions in the discharge tube. The amplitude readings obtained in this phase of the experimental work were made with both a calibrated oscilloscope and a vacuum tube voltmeter. The agreement with the values indicated by Fowler lends strong credence to that portion of the hypothesis that deals with striations in the positive column, as will be shown in succeeding sections of this chapter.

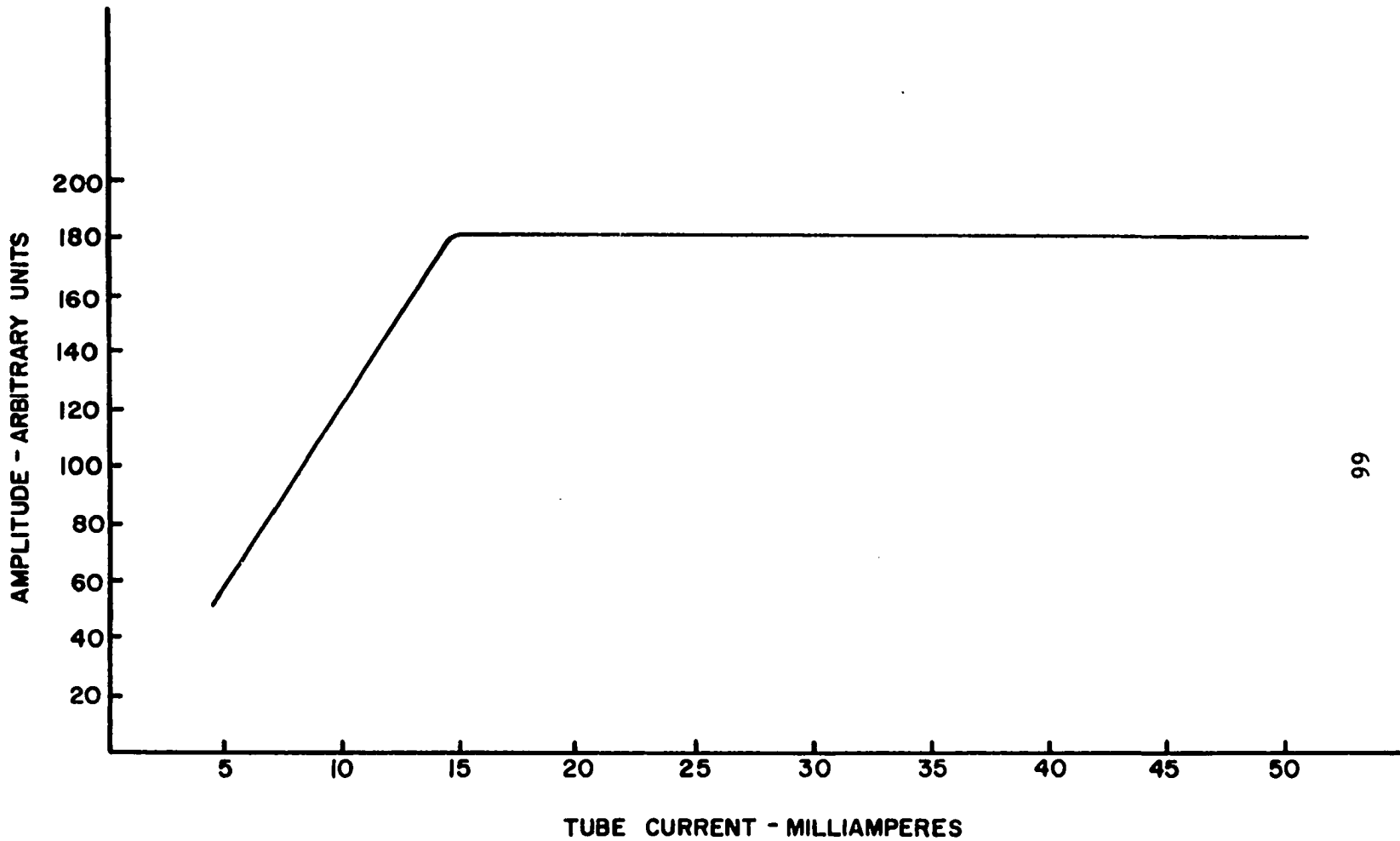
The frequency of occurrence of these waveforms has been found to be an aperiodic function in time. The variation can be related to tube current and has been found to vary from a few per second at low tube currents to several hundred per second at high tube currents. As previously mentioned, the wave-

shape maintains a constant form as a function of tube current after this current has reached the transition value. The frequency of occurrence shows no such characteristic, but rather shows an increase with increasing values of tube current. The manner in which the relative voltage amplitude varies as a function of tube current is exhibited in Figure 17. The variation of the rate of occurrence has been plotted and is in a later section which deals more extensively with the recurrence rates (see Figure 25).

Exterior Probe Waveforms

The characteristic waveform of the signal from the exterior probe is shown in Figure 15. An analysis of these waveshapes yields a time to rise from zero to maximum value of less than 30×10^{-9} seconds. The time required for the wave to decay to its minimum level is 10 microseconds. The rise time of this voltage was found to be independent of tube current and pressure. If the wave occurred at all, the rise time was at least as fast as the oscilloscope. The decay time was determined to be a function of the current in the discharge tube until the aforementioned transition points occurred. The transition points for the exterior signal were the same as those observed for the interior signal (i.e., 14 milliamperes at 400 microns mercury and 37 milliamperes at 1000 microns mercury).

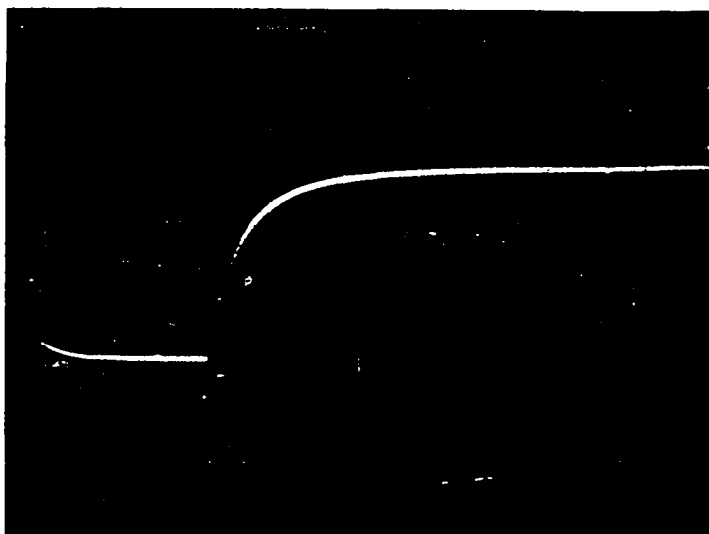
The waveforms exhibited in Figure 18 are typical of the results obtained for all currents above the transition current. The variation of the relative magnitude and decay time as a function



AMPLITUDE VARIATION vs TUBE CURRENT INTERIOR
PROBE

P = 450 μ Hg

FIGURE 17



T = 2 Microseconds/cm

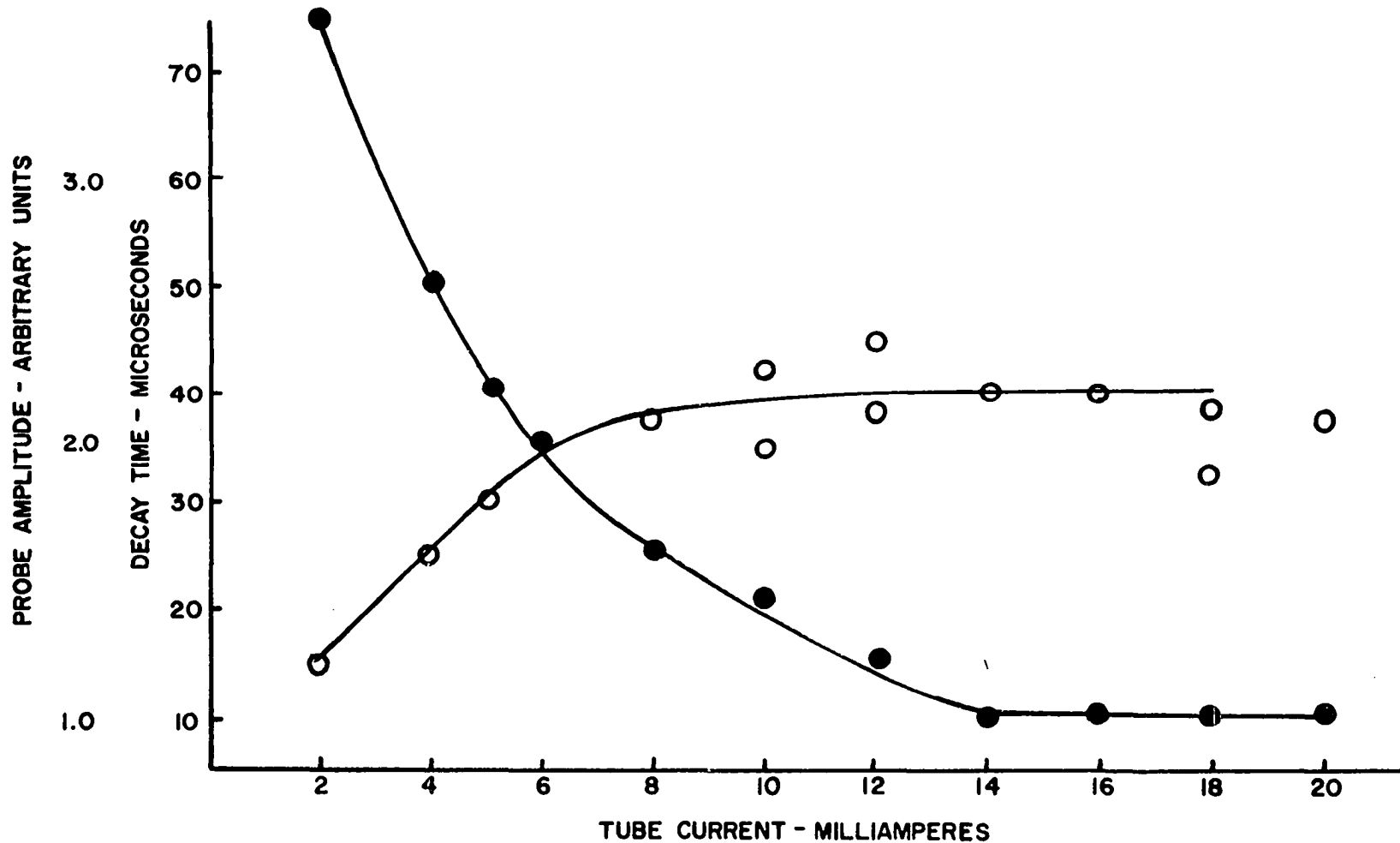
A = .1 volts/cm

EXTERIOR PROBE WAVESHAPE

Figure 18

of tube current is shown in Figure 19 while the supporting data appear in Table 1. To support the hypothesis more than just a waveshape must be presented and the items necessary to provide this support are as follows:

1. The source of the induced field must be isolated and compared to the location postulated in the hypothesis as being that portion of the discharge giving rise to the wave.
2. Attempt to relate the steady signal value duration to the distance between the positive space charge region and the negative glow.
3. Evaluate the exponent of equations (73) and (75).
4. Ascertain if the frequency of occurrence of the interior and exterior waves could be correlated.
5. Attempt to determine the magnitude.
6. Determine if the same waveshapes appeared at each probe.



VARIATION OF DECAY TIME AND AMPLITUDE vs TUBE CURRENT FOR CONSTANT PRESSURE AND A SINGLE POSITION

FIGURE 19

TABLE 1

VARIATION OF RELATIVE AMPLITUDE AND DECAY TIME

Tube Current Milliamperes	<u>Exterior Probe</u>			
	Rise Time Microseconds	Dwell Time	Decay Time	Amplitude Arbitrary
2	*	+	75	1.2
4	*	+	50	1.6
5	*	+	40	1.8
6	*	+	35	2.0
8	*	3	25	2.1
10	*	6	21	2.0
12	*	5	15	2.4
14	*	7	10	2.2
16	*	7	10	2.2
18	*	5	10	1.9
20	*	6	10	2.1
22	*	8	10	2.3

This table was compiled from data taken at constant pressure and at a single position along the tube. This position was that which gave maximum signal strength for the pickup system and was found to lie near the center of the cathode fall region dark space.

*Rise time could not be determined from this information since it was faster than the oscilloscope trace at these settings.

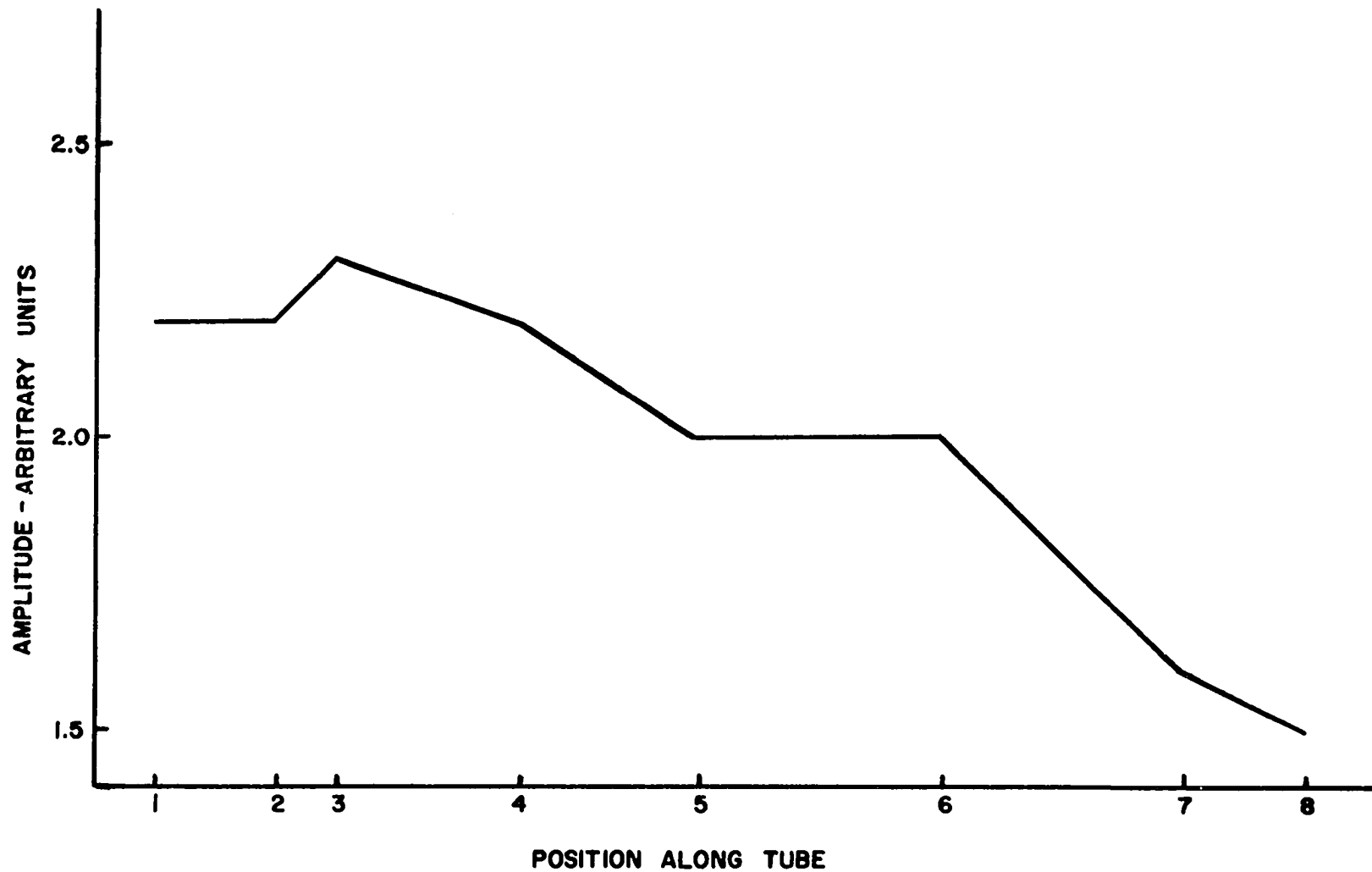
+No dwell time was apparent when the decay time was to be determined for these tube currents.

Location of the source.--The location of the region of the gaseous discharge producing the wave was found by two techniques. First, the exterior probe was moved along the tube and the relative amplitude recorded. These results clearly show that the maximum amplitude position was directly over the cathode dark space. The results are shown in Figure 20, while the data appears in Table 2. The second method used was to place the pickup at the point determined by the first method and then to electromagnetically isolate the tube from the probe. This was accomplished by placing a shielding plate between the tube and the probe and moving this plate toward the probe from both ends of the tube. The results of this investigation are shown in Figure 21. This figure shows that a well defined region exists acting as a source for the observed waveforms. This region can be visually observed to coincide with the cathode fall region as shown in Figure 7. The experimental results show that the characteristics of these waveforms are essentially the same over a wide variety of parameter variations and serves to substantiate the postulation that the cause is related to the charge of the ion rather than the mass of the ion.

Relation of signal to cathode dark space.--Loeb (21) has reported that the average gradient in the cathode dark space for air discharges in the pressure ranges used is approximately 10 volts per cm. A first order approximation of the velocity of N_2^+ ions

in this region is

$$\bar{v} = \sqrt{\frac{2q}{M} (\bar{E} \cdot d)}$$



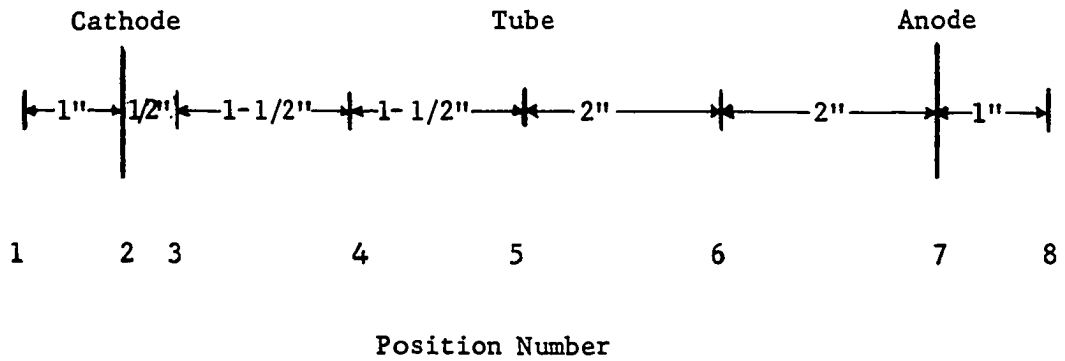
AMPLITUDE VARIATION AS A FUNCTION OF PROBE POSITION

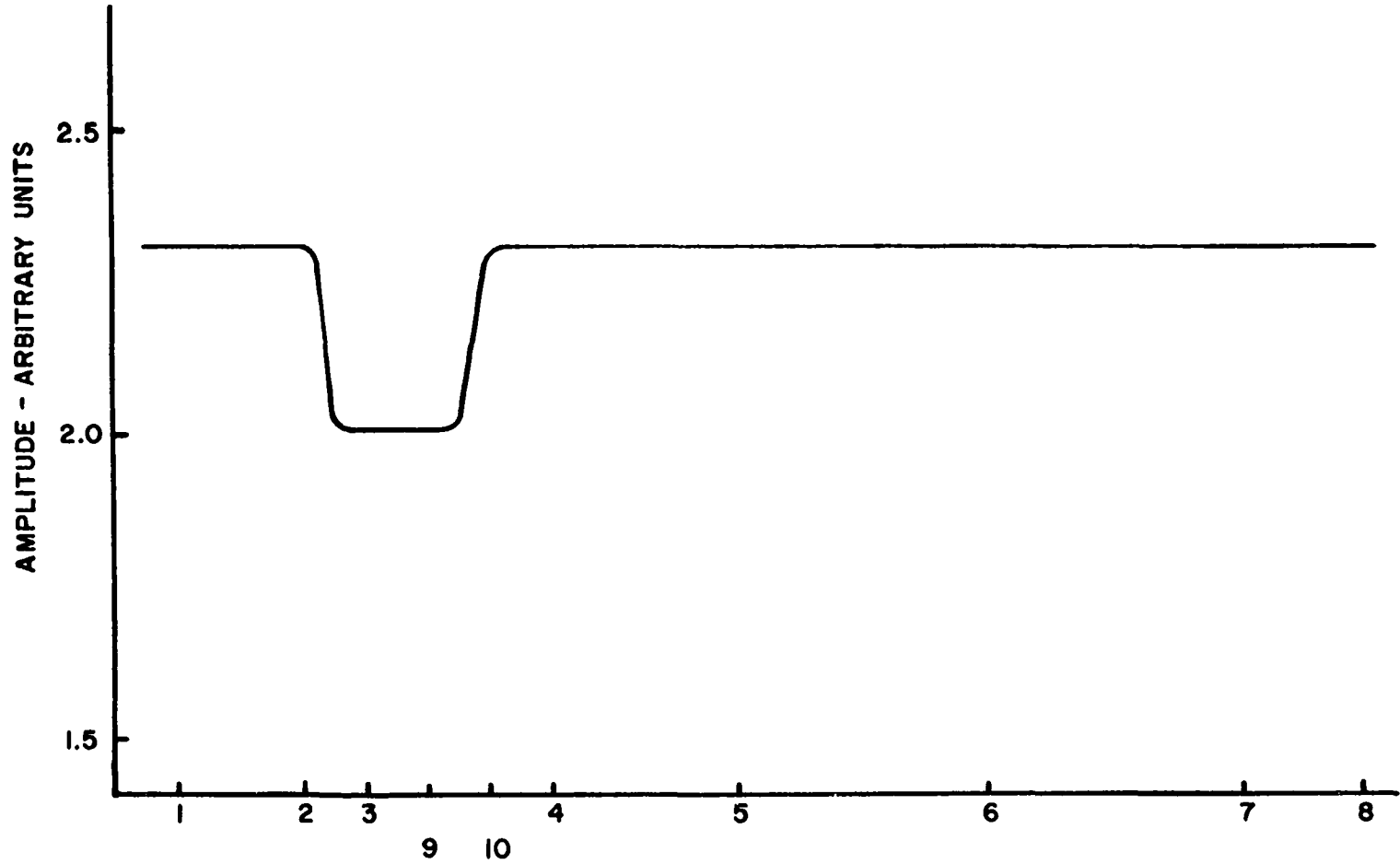
FIGURE 20

TABLE 2

VARIATION OF SIGNAL LEVEL AS A FUNCTION OF POSITION ALONG THE TUBES

<u>Exterior Probe</u>		
Position	Amplitude	Tube Current
1	2.2	40
2	2.2	40
3	2.3	40
4	2.2	40
5	2.0	40
6	2.0	40
7	1.6	40
8	1.5	40





POSITION ALONG THE TUBE
AMPLITUDE VARIATION AS A FUNCTION OF POSITION OF A SHIELDING PLATE ALONG THE TUBE

FIGURE 21

where M = mass of the ion

q = charge of the ion

\bar{E} = electric field

d = distance of travel

thus

$$\bar{v} = 5.7 \times 10^4 \text{ meters per second}$$

The dwell times from Figure 19 are seen to be 4×10^{-6} seconds and 3.5×10^{-6} seconds. This indicates a cathode dark space of from 2.0 cm to 2.3 cm. This is in reasonably good agreement with the value given by von Engel (31) of approximately 2.5 cm and compares favorably with the visually observed values of 2.3 cm. The maximum dwell time observed was 8×10^{-6} seconds, and the minimum 3×10^{-6} seconds. This gives a maximum cathode dark space value for the N_2^+ ions as 4.6 cm. If, as was postulated, the dwell time is mass dependent, this could well be the effect of CO_2^+ or NO_2^+ which would lower the maximum length to approximately 3 cm which again is in reasonably good agreement with theory. The calculations with Argon show more nearly a constant value of dwell time, as compared to air. The dwell time showed a value of 2.2 cm which agrees, within experimental error, with that given by von Engel (31) as approximately 2.1 cm. Note that these calculations are a first order approximation only.

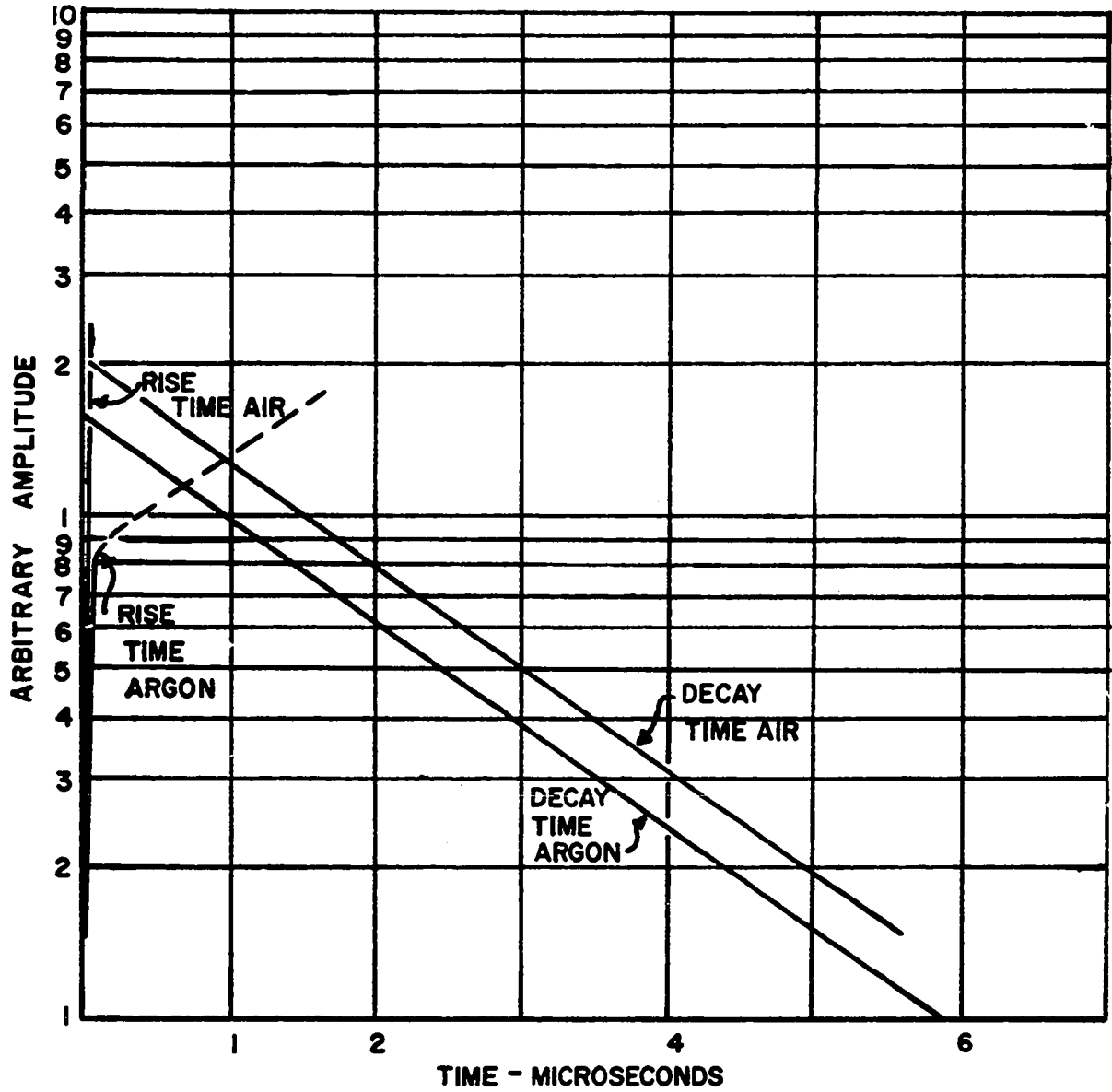
Exponent evaluation.--The evaluation of the exponents of the exponential terms of equations (70) and (72) is most easily accomplished by plotting the decay times and evaluating the slope.

The significance of the rise time, as found in this investigation, is that of a maximum value, since it is at least as fast as the measuring equipment. A plot of the decay time is shown in Figure 22. As was brought out in the hypothesis, the manner in which the energy of the positive ions is given up should be very nearly the same, once the positive space charge region is fully established. This concept was tested by flushing the tube with pure Argon and measuring the same parameters as measured for air. As is evident from Figure 22, the slope of the two curves is the same, while the amplitude on the same relative scale is less for Argon than for air. The exponents are as follows:

$$\xi \approx 30 \times 10^{+9} \text{ (seconds)}^{-1} \text{ (minimum value)}$$

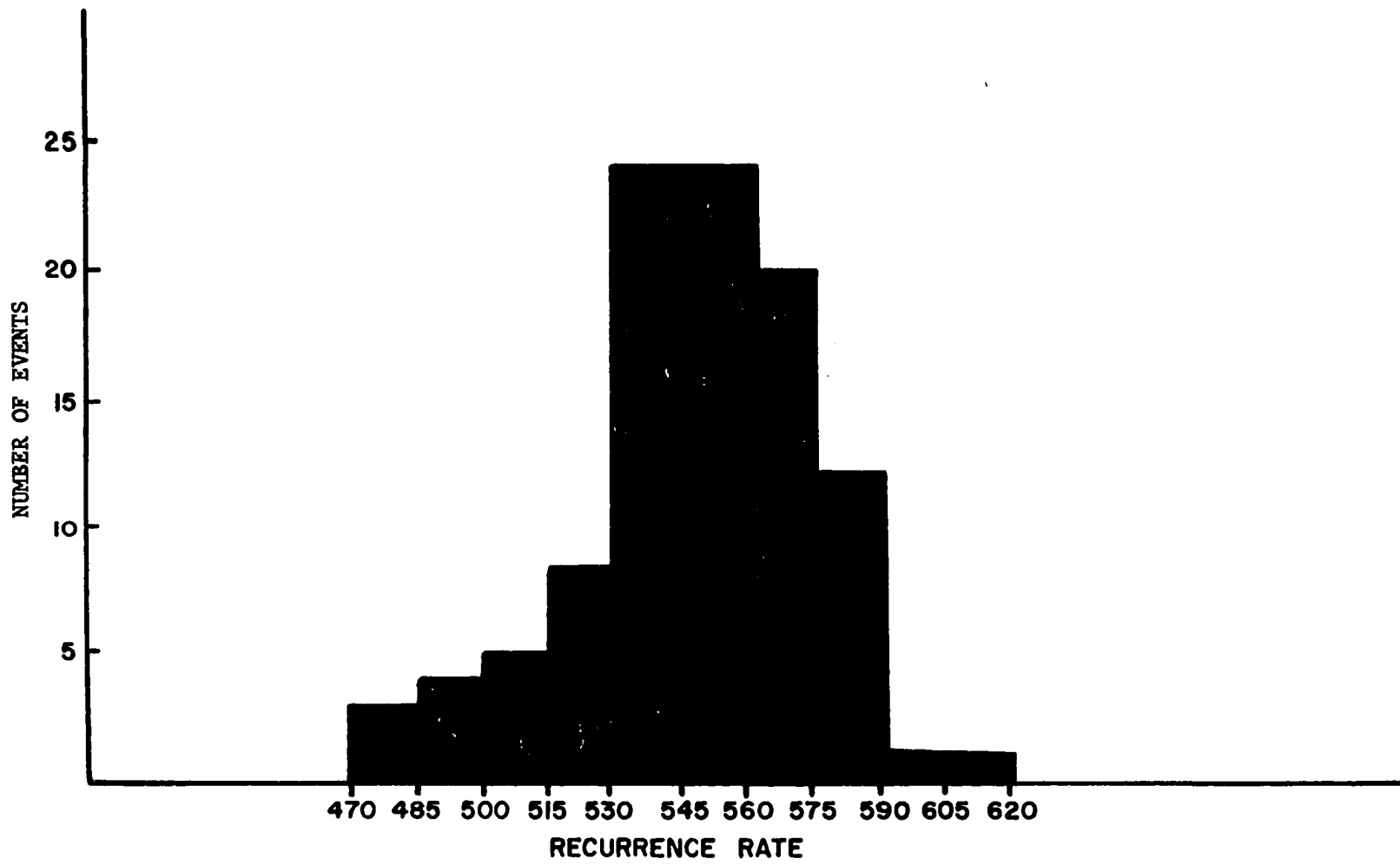
$$\psi = 3 \times 10^6 \text{ (seconds)}^{-1}$$

Recurrence correlation.--According to the hypothesis, the striations and the exterior induced field waves are caused by the same stimulus. If such is the case, then it was stated that a high correlation coefficient should be found between the two rates of occurrence. Since the rate of recurrence is presumed to be a random rate as dictated by a Maxwellian velocity distribution, a large number of samples was deemed necessary. A sampling was made for several values of tube currents and constant tube pressures. These values are presented in Tables 5 and 6 of Appendix C. Typical of this data is that accumulated at 80 milliamperes which is depicted in bar graph form in Figures 23 and 24. The tabulated data for the correlation coefficient calculation is given in Table 3.



AMPLITUDE AS A FUNCTION OF TIME FOR EXTERIOR PROBE
IN AIR AND ARGON

FIGURE 22



RECURRENCE RATE OF INTERIOR PROBE SIGNAL $I_t = 80$ ma $P = 450 \mu$ Hg

FIGURE 23



RECURRENCE RATE OF EXTERIOR PROBE SIGNAL $I_t = 80 \text{ ma}$ $P = 450 \mu \text{ Hg}$

FIGURE 24

TABLE 3

CORRELATION COEFFICIENT CALCULATION DATA

0.1 x	N	T	0.1 y	N	T
<u>+7</u>	1	49	<u>+7</u>	4	196
<u>+6</u>	6	216	<u>+6</u>	2	72
<u>+5</u>	3	75	<u>+5</u>	5	125
<u>+4</u>	6	96	<u>+4</u>	6	96
<u>+3</u>	24	216	<u>+3</u>	15	135
<u>+2</u>	22	88	<u>+2</u>	25	100
<u>+1</u>	30	30	<u>+1</u>	30	30
0	<u>11</u>	<u>0</u>	0	<u>16</u>	<u>0</u>
	103	770		103	754

From the above tabulated data the following are found

$$N = 103$$

$$N\sum x^2 = 770$$

$$N\sum y^2 = 754$$

$$xy = 625$$

The correlation coefficient is

$$r^2 = \frac{[N\sum xy - \sum x \sum y]^2}{[N\sum x^2 - (\sum x)^2] [N\sum y^2 - (\sum y)^2]}$$

which after substitution and reduction becomes

$$r = \frac{67030}{69606} = \underline{0.963}$$

This coefficient gives an indication that correlation exists between the recurrence rate registered on the interior probe

and that found for the exterior probe.

It is interesting to note that the recurrence rates obtained by the counting method and reduction technique show a consistent trend as a function of tube current. This difference is in direct opposition to results reported in reference (21), which states that striations going toward the anode occur at a more rapid rate than those going toward the negative regions. The results are shown graphically in Figure 25, while the reduced data are given in Table 4.

TABLE 4

RECURRENCE RATE SUMMARY AND CALCULATIONS

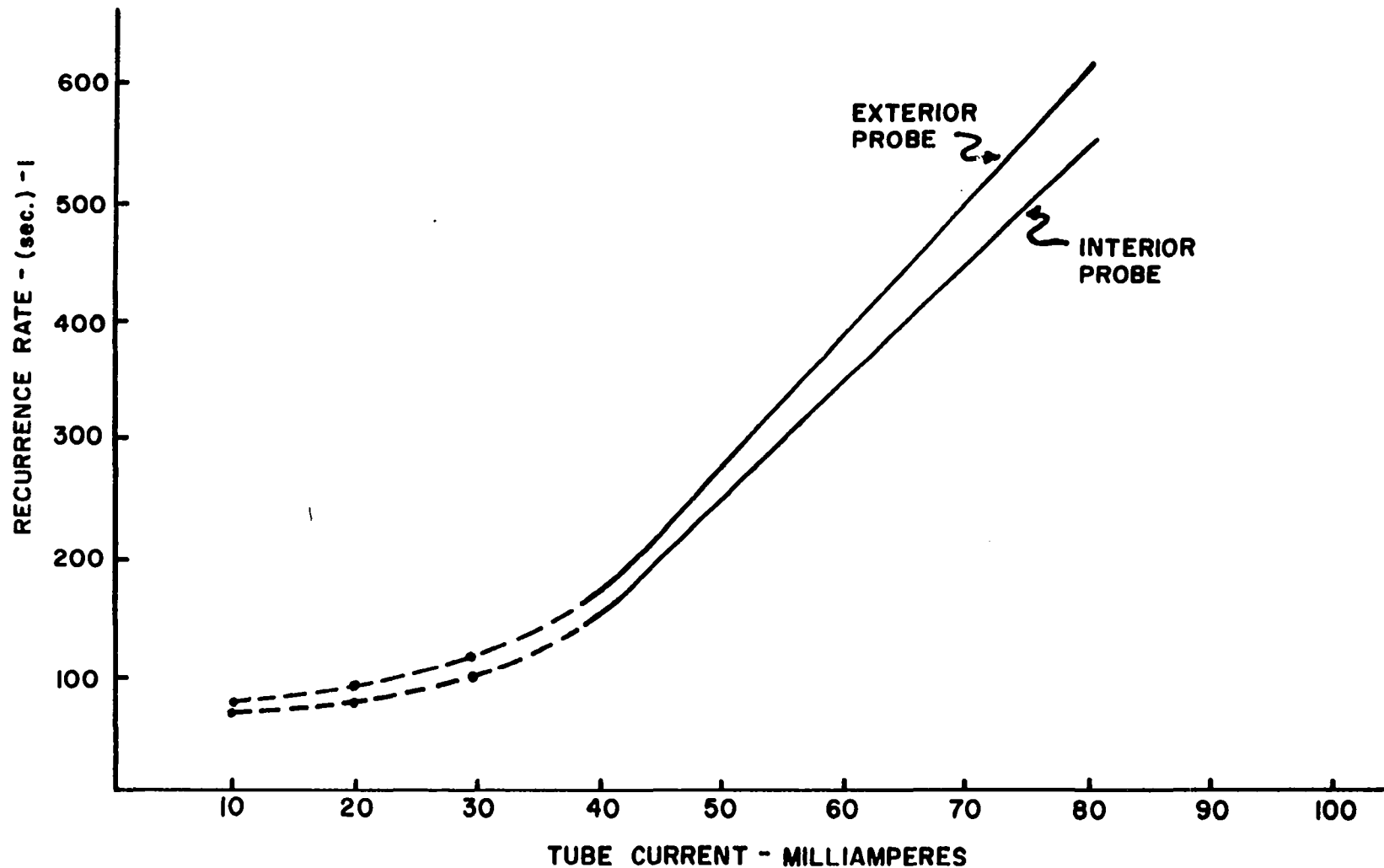
Exterior	Interior
$I_t = 10 \text{ ma}$	$I_t = 10 \text{ ma}$
$N = 37$	$N = 37$
$\sum ()^2 = 190109$	$\sum ()^2 = 180463$
$RMS = \sqrt{5138.08}$	$RMS = \sqrt{4877.38}$
Recurrence Rate = $72 \frac{\text{events}}{\text{second}}$	Recurrence Rate = $70 \frac{\text{events}}{\text{second}}$
$I_t = 20 \text{ ma}$	$I_t = 20 \text{ ma}$
$N = 37$	$N = 37$
$\sum ()^2 = 311909$	$\sum ()^2 = 197277$
$\sum () = 3377$	$\sum () = 2699$
Ave = 91 events/sec	Ave = 73 events/sec
$RMS = \sqrt{8429.97}$	$RMS = \sqrt{5331.81}$
Recurrence Rate = 92 events/sec	Recurrence Rate = 73 events/sec

TABLE 4 (continued)

$I_t = 40 \text{ ma}$	$I_t = 40 \text{ ma}$
$N = 36$	$N = 36$
$\sum ()^2 = 1017818$	$\sum ()^2 = 825261$
$\sum () = 6046$	$\sum () = 5349$
Ave = 169 events/sec	Ave = 151 events/sec
$\text{RMS} = \sqrt{28272.72}$	$\text{RMS} = \sqrt{22923.92}$
Recurrence Rate = 168 events/sec	Recurrence Rate = 151 events/sec
$I_t = 60$	$I_t = 60$
$N = 37$	$N = 37$
$\sum ()^2 = 5903510$	$\sum ()^2 = 4679905$
$\sum () = 14758$	$\sum () = 13139$
Ave = 399 events/sec	Ave = 355 events/sec
$\text{RMS} = \sqrt{159554.32}$	$\text{RMS} = \sqrt{126483.39}$
Recurrence Rate = 399 events/sec	Recurrence Rate = 356 events/sec
$I_t = 80 \text{ ma}$	$I_t = 80 \text{ ma}$
Recurrence Rate = 612 events/sec	Recurrence Rate = 547 events/sec

Summary

Exterior Rate	I_t	Interior Rate
72	10	70
92	20	73
168	40	151
399	60	356
612	80	547



RECURRENCE RATE COMPARISON FOR INTERIOR AND EXTERIOR PROBES

FIGURE 25

While these results are given in support of the hypothesis, it is felt that a more definitive measurement should be made of the recurrence rates. A measurement of the striations using the same technique as that reported in reference (21) should be made simultaneously with those as measured in this program.

Other information obtained from the data reduction around the 80 milliampere point include the following:

Exterior Probe		Interior Probe
612 events/sec	Most Probable Rate	547 events/sec
$\sigma_x = 24.4$	Standard deviation	$\sigma_y = 26.9$

Magnitude.--The manner in which the amplitude varied was found to be dependent upon the geometry of the probe. Thus, no definitive statement concerning the amplitude can be made.

Waveshape Comparison.--Examination of Figures 14 and 15 shows that there is no comparison of the two waveforms. A close analysis of the output of the interior probes showed that a waveform of the type induced in the exterior probe could be seen; however, this signal was so far down in the noise that no conclusive evidence could be obtained. At no time did a waveshape characteristic of the interior probe appear on the exterior probe. From these observations it was determined that the waveforms were the result of two distinct phenomena occurring in the tube. The interior caused by striations in the positive column and the exterior a result of the positive ion swarm going toward the cathode.

In order to check these results a probe was placed in the cathode

fall space of the discharge and the waveforms observed. These results showed a shape identical with the interior positive column measurements. This indicates that the current pulsations are so much greater in magnitude, that it is impossible to have observed the hypothesized phenomenon without an exterior probe in the induction field of the discharge.

Far Field Measurements

The far field measurements made as a part of this program were of a primitive variety. A check of the emission signals was made by sweeping frequencies in the VHF to microwave bands of 200 kilocycles to 35 kilomegacycles per second. The results indicated that the signals generated by the plasma were truly white noise or that any genuine characteristic signature was well below the noise environment of the surrounds. As a consequence, no further measurements were made of the far field emission characteristics.

CHAPTER VII

CONCLUSIONS

A hypothesis has been presented to explain the appearance of a relaxation waveshape postulated to be caused by processes in the negative glow region. A number of pertinent points have been presented that were satisfied experimentally. These points are presented as conclusions to the program.

1. The location of the source of the signal observed was postulated to be located in the cathode fall region. The results of this investigation show that this postulation is true. The source has been conclusively located in this region of the discharge.
2. It was postulated that the signals of the positive column were from striations which were generated as a result of the ionizing collisions in the negative glow. Further, a relationship should exist between the rates of occurrence of these waves. Evidence was observed in the form of relative amplitudes in the positive column that shows the possible connection between the waves on the interior probe and positive column striations. A correlation coefficient calculation between the rates of occurrence yields a value of sufficient magnitude to

justify this assumption. In addition, the difference in the rates from outside to inside were of the same direction and the standard deviation is satisfied by a Maxwellian velocity distribution.

3. It was hypothesized that the duration of the steady signal from the cathode dark space should be related to the length of this region. A first order approximation shows good agreement.
4. The decay time of the exterior wave should be connected with the density of positive ions in the positive space charge sheath surrounding the cathode. The exponent was found to be 3×10^6 per second. According to Loeb (21), the best experimental value for this type of exponent is of the order of 1.5×10^6 per second.

It may be concluded that sufficient experimental support has been supplied to warrant a hypothesis of this type. It has been shown that the type of evidence given in support could not have been obtained through investigation of the glow discharge by observation made by interaction with light beams, insertion of probes into the discharge region, or analysis of the fluctuations in the volt-ampere characteristic.

The only variance with present theory and experiment lies in the relative recurrence rates between positive and negative going striation and magnitude of these rates.

CHAPTER VIII

RECOMMENDATIONS

The experimental and theoretical work performed have led to many interesting possibilities in the field of gaseous electronics. The experimental program was designed to obtain maximum usage from the available equipment. As a result, several areas of direct interest are not supported due to this fundamental equipment limitation.

As examples, the following areas are noted as having rather severe equipment limitations and very definitely in need of further development:

1. The rise time of the wave that was postulated to occur at the boundary of the negative glow region could not be determined due to limitations on the equipment. Oscilloscopes now commercially available are capable of performing this task.
2. The correlation between the interior and exterior waves is in need of further exploration. The data taken was obtained with a single electronic counter. To bring about a better correlation the data should be observed at the same time. The only justification for obtaining the correlation factor reported is that the rates were found to

vary in the same manner about the most probable value by observing oscilloscope tracings.

3. The power supply and vacuum system leave a lot to be desired from the standpoint of control and versatility. A more positive control system on the pressure would have given better data in a much shorter period of time.
4. The tube itself is constructed from a plexiglass pipe. As a result the maximum long-time (one hour) current capability is approximately 90 milliamperes. Above this value the tube begins to soften with the rather obvious consequences. A higher current capability would allow the hypothesis to be checked out over a much broader range of parameters.
5. Light sensing equipment, as photometers and spectrometers, would enable an experiment to be run to determine the validity of the results on recurrence rates as well as check the postulation concerning positive column striations. This equipment would also permit a better definition of the cathode dark space for the particular tube used, thus giving another check on the hypothesis with regard to the constant amplitude signal. A whole series of further investigations have been proposed to aid in either validating or invalidating the hypothesis presented in this dissertation.

ANOTATED BIBLIOGRAPHY

1. Bachynski, M. P., "Plasma Physics - An Elementary Review" Proceedings of the I.R.E., Vol. 49, no. 12, December 1962.
2. Bishop, A., Project Sherwood, Addison-Wesley Book Co., Inc., Reading, Mass., 1958.
3. Busemann, A., "Is Aerodynamics Breaking an Ionic Barrier," Electromagnetic and Fluid Dynamics of Gaseous Plasma, Polytechnic Press, New York, 1962.
4. Chen, Kun-Mu, "Non-linear Electrical Conductivity of a Fully Ionized Gas," I.R.E. Transactions on Antennas and Propagation, Vol. AP-10, no. 1, January 1962.
5. Chodorow, M. and G. S. Kino, Research on Plasma Boundary Studies, Report Number 963, Microwave Laboratory, W. W. Hansen Laboratories of Physics, Stanford University, Stanford, California, October 1962.
6. Cloutier, G. G., M. P. Bachynski, and K. A. Graf, "Antenna Properties in the Presence of Ionized Media," "Research Report 7-801-16, Research Laboratories, RCA Victor Co. Ltd., Montreal, Canada, March 1962.
7. Cobine, James Dillon, Gaseous Conductors, Dover Publications, Inc., New York, 1958.
8. Drummond, J. E., "Microwave Propagation in Hot Magnetic Plasmas" Physics Review, Vol. IIV, 1958.
9. Drummond, J. E., Plasma Physics, McGraw-Hill Book Co., Inc., 1961.
10. Drummond, J. E., "Transconductance Properties of Plasma," I.R.E. Transactions in Antennas and Propagation, Vol. AP-10. no. 1, (1962).
11. Donahue, T. and G. H. Dieke, "Oscillatory Phenomena in Direct Current Glow Discharges," ASTIA AD-134792, 1948.
12. Flock, W. L. and R. S. Elliott, "The Radiation Pattern of a Microwave Horn and a Plasma Layer," I.R.E. Transactions on Antennas and Propagation, Vol. AP-10, no. 1 (1962), pp. 69-78.
13. Fowler, R. G., Personal Communication.
14. Fried, B. D., M. Gell-Mann, J. D. Jackson, and H. W. Wyld, "Longitudinal Plasma Oscillations in an Electric Field" Journal of Nuclear Energy: Part C, Vol. 1, no. 4, July 1960.

15. Haus, H. A., "Noise in One-Dimensional Electron Beams" J. Applied Physics, Vol. 26 (1955) p. 560.
16. Hessel, A., N. Marcuvitz, and J. Shmoys, "Scattering and Guided Waves at an Interface Between Air and a Compressible Plasma," I.R.E. Transactions on Antennas and Propagation, Vol. AP-10 no. 1, January 1962.
17. Hessel, A. and Shmoys, J., "Excitation of Plasma Waves by Dipole in a Homogeneous Isotropic Plasma," Electromagnetic and Fluid Dynamics of Gaseous Plasma, Polytechnic Press of the Polytechnic Institute of Brooklyn, (1962) pp. 173-183.
18. Hodara, H., "The Use of Magnetic Fields in the Elimination of Re-entry Radio Blackout" Proceedings of the I.R.E., Vol. 49, no. 12, December 1961.
19. Jackson, J. D., "Longitudinal Plasma Oscillations" Journal of Nuclear Energy: Part C, Vol. 1, no. 4, July 1960.
20. Linhart, J. G., Plasma Physics, North-Holland Publishing Co., Inc., Amsterdam, Interscience Publishers, Inc., New York, 1961.
21. Loeb, L. B., Basic Processes of Gaseous Electronics, University of California at Los Angeles Press, Los Angeles, California, 1955.
22. Newstein, M and J. Lurye, "The Field of a Magnetic Line Source in the Presence of a Layer of Complex Refractive Index." Report No. 1, Technical Research Group, New York, 1956.
23. Panofsky, W. R. H. and M. Phillips, Classical Electricity and Magnetism, Addison-Wesley Publishing Co., Inc. Reading, Mass., 1956.
24. Raemer, H. R., "Radiation from Linear Electric or Magnetic Antennas Surrounded by a Spherical Plasma Shell" I.R.E. Transactions on Antennas and Propagation, Vol. AP-10, no. 1 (1962)
25. Rose, D. J. and M. Clark, Jr., Plasmas and Controlled Fusion, John Wiley and Sons, Inc., New York, 1961.
26. Smythe, W. R., Static and Dynamic Electricity, McGraw-Hill Co., Inc., New York, 1950.
27. Stix, Thomas Howard, The Theory of Plasma Waves, McGraw-Hill Book Co., New York, 1962.
28. Stratton, J. A., Electromagnetic Theory, McGraw-Hill Book Co., Inc., New York, 1941.

29. Tamir, T. and A. A. Oliner, "The Influence of Complex Waves on the Radiation Field of a Slot-Excited Plasma Layer" I.R.E. Transactions on Antennas and Propagation, Vol. AP-10, no. 1, January 1962.
30. Trivelpiece, A. W., "Slow Wave Propagation in Plasma Waveguides" TR-7 Electron Tube and Microwave Laboratory, California Institute of Technology, May 1958.
31. von Engel, A., Ionized Gases, Oxford University Press, Oxford, England, 1955.
32. Wait, J. R., "The Electromagnetic Field of a Dipole in the Presence of a Thin Plasma Sheet," Applied Scientific Research, Vol 8, Sect. B, 1961.
33. Wharton, C. B., "General Plasma Diagnostic Studies," RISO Report, Danish Atomic Energy Commission, November 1960.

References Not Specifically Noted in the Text

- Abele, M., "Radiation in a Plasma from a Uniformly Moving Distribution of Electric Charge," Electromagnetics and Fluid Dynamics of Gaseous Plasma, Polytechnic Press, New York, 1962.
- Alfven, H., Cosmical Electrodynamics, Oxford University Press, 1950.
- Astrom, Ernst, "On Waves in an Ionized Gas" Arkiv For Fysik, Band 2, nr42, 7 June 1960.
- Bohm, D. and E. P. Gross, "Theory of Plasma Oscillations" The Physical Review, Vol. 75, no. 12, 1949.
- Brown, Sanborn C., Basic Data of Plasma Physics, The Technology Press of MIT and John Wiley and Sons, Inc., New York, 1959.
- Chapman, S. and T. G. Cowling, The Mathematical Theory of Non-Uniform Gases, Cambridge University Press, 1939.
- Clauser, F. H., Symposium of Plasma Dynamics, Addison-Wesley Publishing Co., Inc., Reading, Mass., 1960.
- Cowling, T. G. Magnetohydrodynamics, Interscience Tracts on Physics and Astronomy No. 4, Interscience Publishers, Inc., New York, 1957.
- Crawford, F. W. and G. S. Kino, "Oscillation and Noise in Low Pressure DC Discharges," Proceedings of the I.R.E., Vol. 49, no. 12, January 1961.
- Delcroix, J. L., Introduction to the Theory of Ionized Gases, Interscience Publishers, Inc., New York, 1960.
- Goubau, G., "Dispersion in an Electron-Atom Mixture under the Influence of an External Magnetic Field," Hochfrequenz-technik und Elektroakustik, Vol. 46, no. 2, 1935, translated by A. Pingell, NRL.
- Hall, J. G., "Shock Tubes, Part II, Production of Strong Shock Waves; Shock Tube Applications, Design and Instrumentation," UTIA Review No. 12, Institute of Aerophysics, University of Toronto, May 1958.
- Helmer, J. C. and R. L. Jepsen, "Electrical Characteristics of a Penning Discharge" Proceedings of the IRE, vol. 49, No. 12, January 1961.
- Jordan, E. C., Electromagnetic Waves and Radiating Systems, Prentice-Hall, Inc., New York, 1950.
- Kerr, D. E., Propagation of Short Radio Waves, Vol. 13, MIT Radiation Laboratory Series, McGraw-Hill Book Co., Inc., New York, 1951.

Kraus, John D., Antennas, McGraw-Hill Book Company, New York, 1950.

Landshoff, R. K. M., Editor, Magnetohydrodynamics; A Symposium, Stanford University Press, Stanford, California, 1957.

Lehnert, B., "Plasma Physics on a Cosmical and Laboratory Scale," Supplemento A-1, Volume XIII, Seric X, Del Nuovo Cimento, No. 1, 1959.

Mitchner, M., Editor, Radiation and Waves in Plasmas, Stanford University Press, Stanford, California, 1961.

Piddington, J. H., "Hydromagnetic Waves in Ionized Gas," Nature, Vol. 176, 1955.

Post, R. F., "Impurity Radiation Losses from a High Temperature Plasma," RISO Report, Danish Atomic Energy Commission, November 1960.

Ramo, S. and J. K. Whinnery, Fields and Waves in Modern Radio, John Wiley and Sons, New York, 1953.

Rosenbluth, M. N., "Synchrotron Radiation," RISO Reports, Danish Atomic Energy Commission, November 1960.

Sengupta, Dipak L., "The Electrical Conductivity of a Partially Ionized Gas," Proceedings of the IRE, Vol. 49, No. 12, January 1961.

Tannenbaum, B. S., "Dispersion Relations in a Stationary Plasma" Raytheon Company, Waltham, Massachusetts, January 1961.

Tatarshi, V. I., Wave Propagation in a Turbulent Medium, McGraw-Hill Book Company, Inc., New York, 1961.

Taylor, Leonard S., "RF Reflectance of Plasma Sheaths," Proceedings of the IRE, Vol. 49, No. 12, January, 1961.

Tonks, L. and I. Langmuir, "Oscillations in Ionized Gases," Physical Review, No. 33, 1929.

Tuck, James L., "Series of Lectures on Physics of Ionized Gases," Office of Technical Services, U. S. Department of Commerce, Washington 25, D. C., 1956. (AEC Contract W-7405-Eng. 36)

Spitzer, Lyman, Jr., Physics of Fully Ionized Gases, Interscience Tracts on Physics and Astronomy, No. 3, Interscience Publishers, Inc., New York, 1956.

Wharton, C. B., Proceedings of the Fourth International Conference on Ionization Phenomena at Uppsala 1959, Amsterdam, North-Holland, (1960) pp. 737-742.

Whitmer, R. F., "Principles of Microwave Interactions with Ionized Media," Microwave Journal, February 1959.

APPENDIX A

Volt-Ampere Characteristics of the Glow-Discharge Tube

A complete set of curves is presented in Figures 27, 28, 29 and 30 to depict the electrical behavior of the tube. These curves were measured in accordance with the method of Chapter IV and are those that were expected.

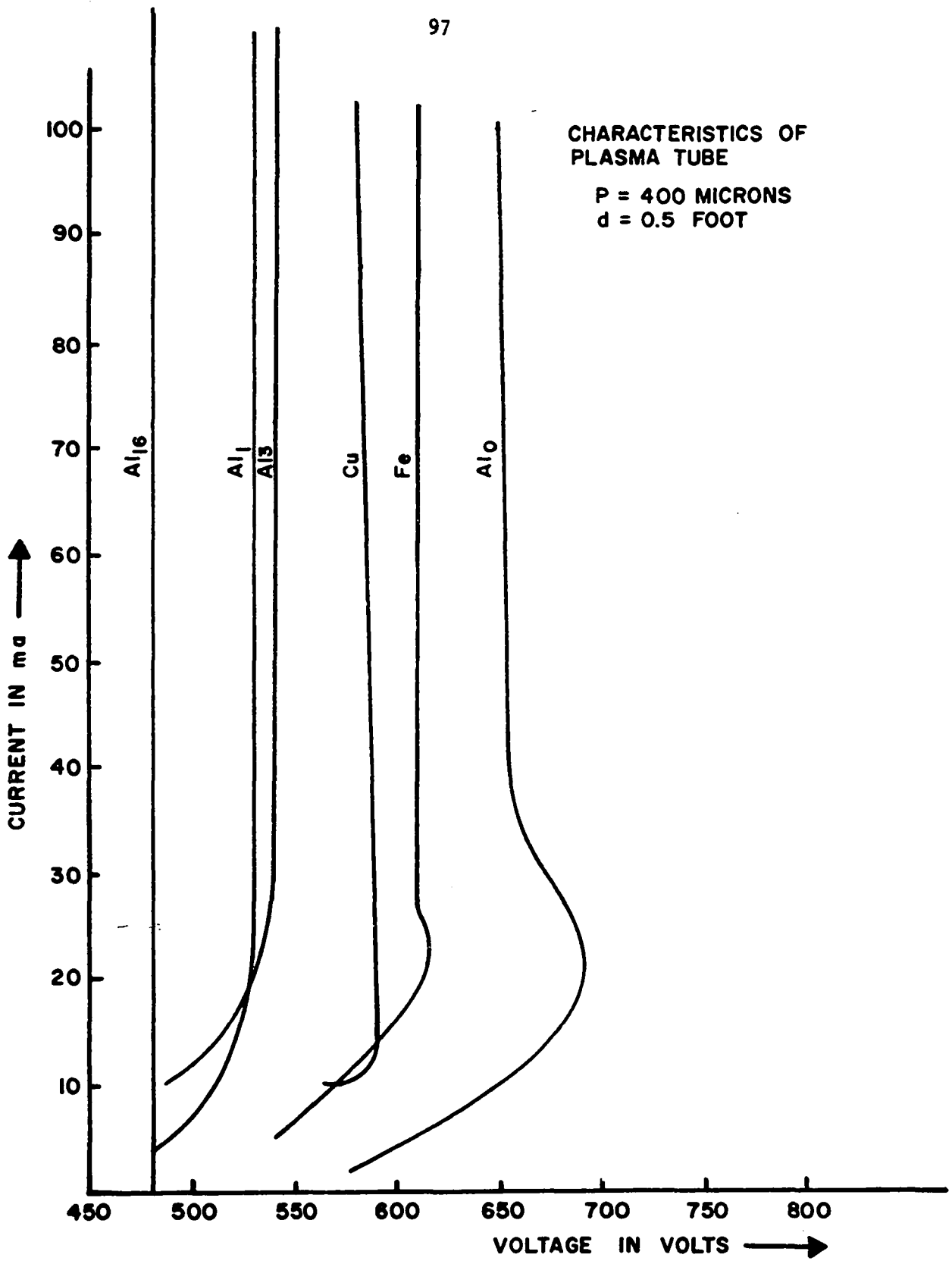
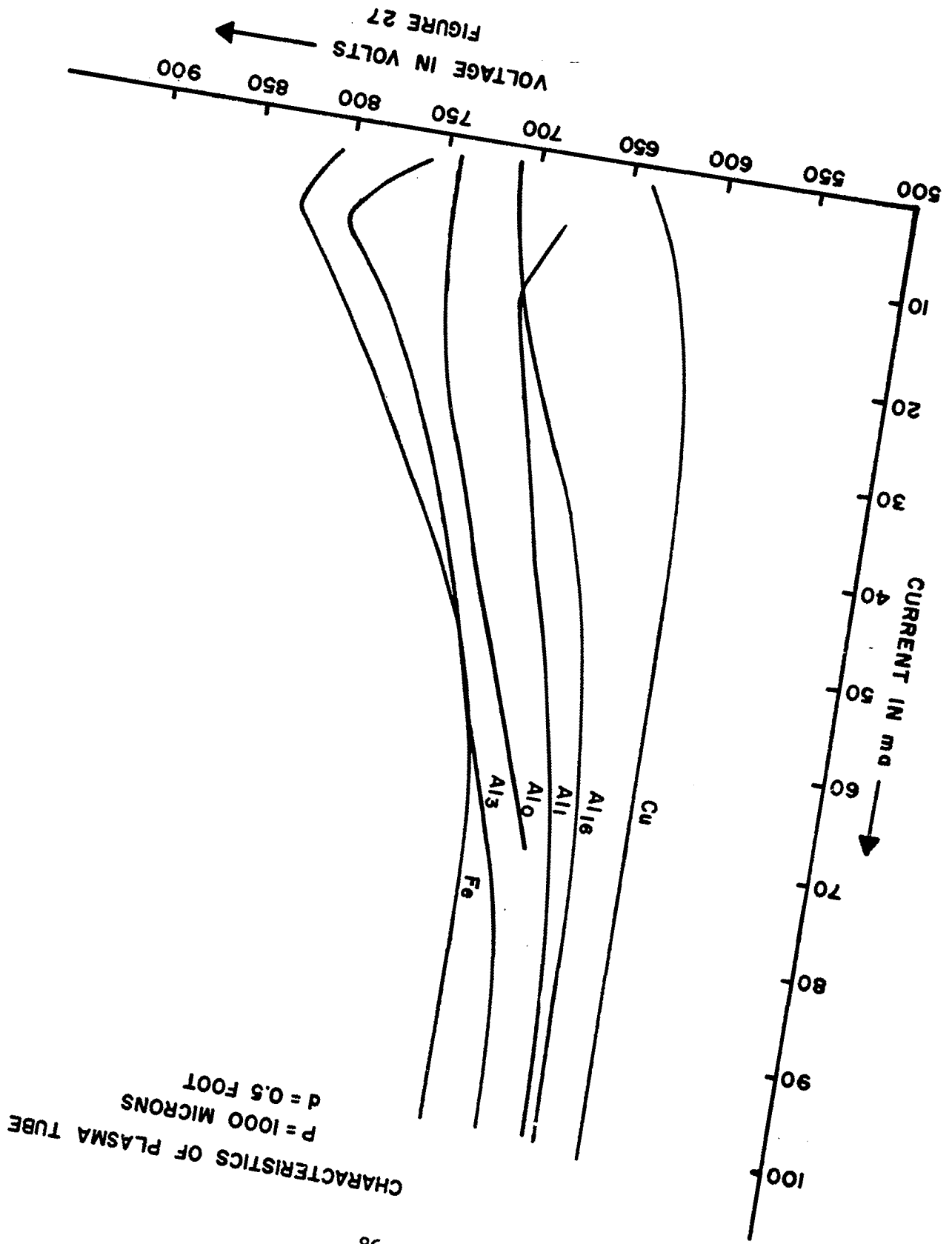


FIGURE 26



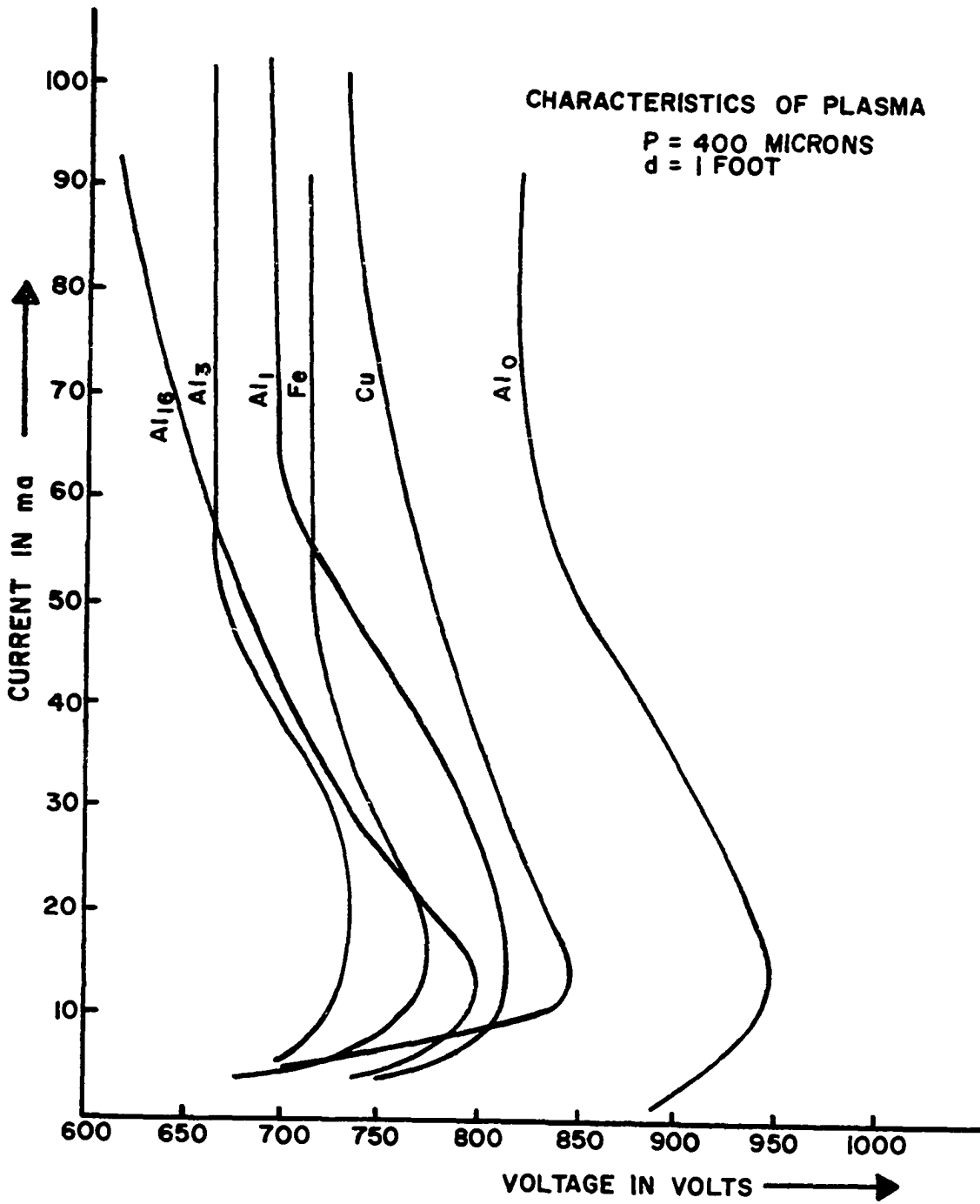


FIGURE 28

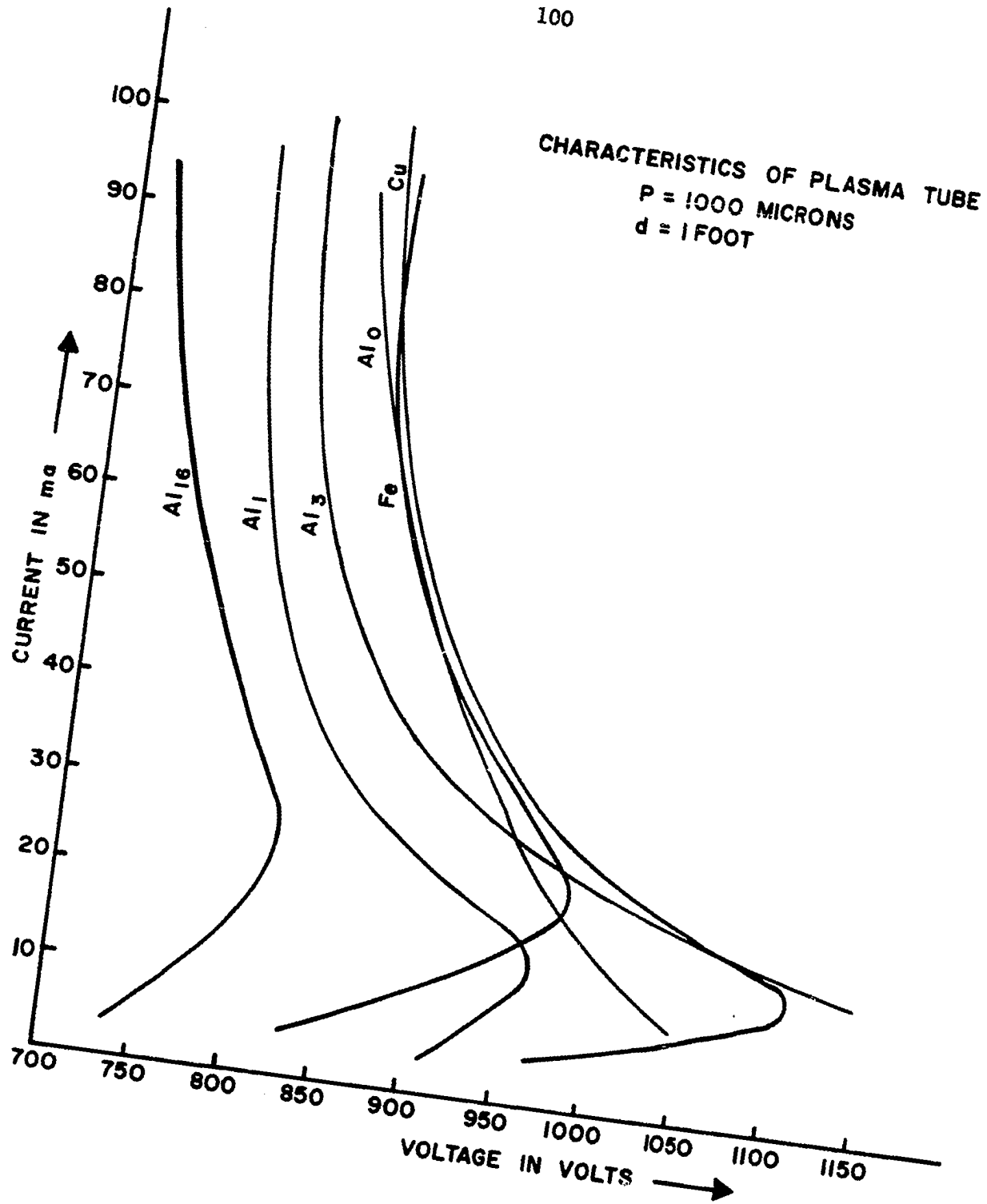


FIGURE 29

APPENDIX B

Bremstrahlung (23, 26, 27)

Bremstrahlung radiation is another possible source of discrete frequency energy which arises from an accelerated charge. To be more specific, bremstrahlung originates from the interaction of ionic and electronic particles which result in an unequal acceleration for each particle due to the mass differences, thus, giving rise to a net acceleration of charge.

At high electron temperatures, on the order of 50 Kev the electron-electron bremstrahlung is not entirely negligible, but no significant radiated power is expected at normal plasma electron temperatures when compared with the ion-electron effect, so a first-order effect due to ion-electron bremstrahlung will be discussed here.

The general radiation field for an accelerated charge has been determined as:

$$E_{\text{rad}} = \frac{q}{4\pi\epsilon_0 s^3 c^2} \left(\bar{r} \times \left[\bar{r}_u \times \dot{\bar{u}} \right] \right) \quad (76)$$

The rate of radiation at any surface of the field is the rate of energy loss radiated into the solid angle representing the surface.

$$- \frac{dU}{dt} d\Omega = \left(\bar{E} \times \bar{H} \right) \frac{dt}{dt'}, r^2 d\Omega \quad (77)$$

where t represents real time and t' is the retarded time.

If some impact parameter b is assumed, then \dot{u} is given by:

$$\dot{u} = \frac{q_i q_e}{4\pi m_e b^2} \quad (78)$$

inserting this expression into the radiation rate equation yields:

$$-\frac{dU}{dt'} = \frac{q_i^2 q_e^4}{96\pi \epsilon^3 m_e^2 b^4 c^3} \quad (79)$$

Assuming an ion density n_i and an impact parameter cross-section of $2\pi b^2$ the total energy loss is found by integrating the following expressions:

$$\frac{dU}{dt'} = \frac{q_i^2 q_e^4 (n_i u_e)}{96\pi \epsilon^3 c^3 m_e^2} \int_{b_{\min}}^{b_{\max}} \frac{2\pi b^2}{u_e b^4} db \quad (80)$$

where b_{\max} is the Debye length Λ_D and b_{\min} is the Compton wavelength of the electron given as:

$$b_{\min} = \frac{h}{2\pi m_e u_e}$$

thus

$$-\frac{dU}{dt'} \Big|_{\text{total}} = \frac{q_i^2 q_e^4 (n_i)}{48\pi^2 c^3 m_e^2} \int_{\frac{h}{m_e \langle u_e \rangle}}^{\Lambda_D} \frac{db}{b^2}$$

$$-\frac{dU}{dt} = -K \left(\frac{1}{\Lambda_D} - \frac{m_e \langle u_e \rangle}{h} \right)$$

where $\langle u_e \rangle$ is the average velocity assuming a Maxwell-Boltzmann distribution of velocity elements.

$$\langle u_e \rangle = \sqrt{\frac{8kT}{\pi m_e}}$$

$$\therefore -\frac{dU}{dt'} = \frac{q_i^2 q_e^4 n_i}{48\pi \epsilon^3 c^3 m_e^2} \left[\frac{2\pi m_e}{h} \sqrt{\frac{8kT}{\pi m_e}} - \frac{1}{\Lambda_D} \right] \quad (81)$$

for $\Lambda_D = \frac{\epsilon kT}{n_e q_e^2} \quad (82)$

$$-\frac{dU}{dt} = \frac{q_i^2 q_e^4 n_i^4}{24\pi\epsilon^3 c^3 m_e h} \sqrt{\frac{8kT}{\pi m_e}} - \frac{q_i^2 q_e^6 n_i^6 n_e}{48\pi^2 \epsilon^4 c^3 m_e^2 kT}$$

From this expression the total power density radiated by all electrons is given by the following equation:

$$W = \frac{q_i^2 q_e^4 n_i^4 n_e}{24\pi\epsilon^3 c^3 m_e h} \sqrt{\frac{8kT}{\pi m_e}} - \frac{q_i^2 q_e^6 n_i^6 n_e}{48\pi^2 \epsilon^4 c^3 m_e^2 kT} \quad (83)$$

Cyclotron or Gyrofrequency Radiation (23, 26, 27)

It has been pointed out that any charged particle subjected to an acceleration would radiate electromagnetic energy. In the case of cyclotron radiation the effect is that of a charge (electron) moving in a circle with the attendant radial acceleration. The application of the results previously obtained present only a first approximation to the actual radiation phenomena, since the derivation was made for a charge free region with constant values of specific inductive capacity and permeability. If a charge is assumed to be moving in a circle of radius "a" with a constant angular velocity, v , then the radiation field and the radiated power density may be calculated by equation (48). Thus:

$$\left[\bar{r}_x (\bar{r}_u \times \bar{u}) \right]^2 = \dot{u}^2 r^4 \left[\left(1 - \frac{u}{c} \cos \theta \right)^2 - \left(1 - \frac{u^2}{c^2} \right) \sin^2 \theta \cos^2 \phi \right]$$

where

$$u = av$$

$$\dot{u} = av^2$$

$$\bar{r}_u = \bar{r} - \frac{\bar{u}r}{c}$$

$$\bar{u} \cdot \bar{r} = \dot{u}r \cos \theta$$

$$\bar{u} \cdot \bar{r} = \dot{u}r \sin \theta \cos \phi$$

φ = azimuthal angle

From which the rate of radiation power density is

$$-\frac{dU(\varphi, \Theta)}{dt'} d\Omega = \frac{e^2 \dot{u}^2}{16\pi^2 \epsilon_0 c^3} \frac{\left(1 - \frac{u}{c} \cos \Theta\right)^2 - \left(1 - \frac{u^2}{c^2}\right) \sin^2 \Theta \cos^2 \varphi}{\left(1 - \frac{u}{c} \cos \Theta\right)^5} d\Omega \quad (84)$$

Integration of equation (75) yields the total rates of radiated energy of a charge 'e' traveling in a circle (orbit) of radius 'a' and angular velocity 'v' as:

$$-\frac{dU}{dt'} = \frac{e^2 \dot{u}^2}{6\pi\epsilon_0 c^3} \frac{1}{\left(1 - \frac{u^2}{c^2}\right)^2} = \frac{e^2 a^2 \omega^4}{6\pi\epsilon_0 c^3} \frac{1}{\left(1 - \frac{u^2}{c^2}\right)^2} \quad (85)$$

with the total power P

$$P = \frac{dU}{dt'} = \frac{e^2 a^2 \omega^4}{6\pi\epsilon_0 c^3} \frac{1}{\left(1 - \frac{u^2}{c^2}\right)^2} \quad (86)$$

The interpretation of the frequency, ω , in this case is that it represents the first order approximation to the cyclotron resonant frequency. From the power relationship it can be seen that the resultant radiation pattern is located in the plane of the orbit, further as the velocity approaches the speed of light the pattern becomes a ray in the forward direction with intensity much greater than any other direction. The frequency spectrum has peaks at ω , 2ω , 3ω ... $n\omega$ and the envelope of these peaks has a broad maximum at

$$\omega = \omega_c \left(1 - \frac{u^2}{v^2}\right)^{-3/2} \quad (87)$$

As was previously mentioned the conditions imposed on the above

calculations are different than those encountered in a plasma region. In the case of a plasma the dielectric constant is different from that of free space and is generally found to be complex. This means that the propagation constant is complex and that the medium is no longer transparent for all frequencies.

Cerenkov Radiation (23, 26, 27)

Since the medium in which the signal generation initiates is taken to be a partially ionized gas, some exploratory considerations of the Cerenkov effect have been done. In this instance, consideration is given to the possibility of radiation being set up by a uniformly moving charge in the dielectric of the plasma.

It is generally quite easy to show that uniformly moving charge in free space does not radiate energy. The relation between the energy U and the momentum of a particle P for a freely moving particle is given by:

$$U^2 = p^2 c^2 + m_0^2 c^4 \quad (88)$$

where m_0 = rest mass of the particle. Differentiating this relation and determining the ratio of momentum change to energy, the following relation is determined:

$$\frac{dp}{dU} = \frac{1}{c} \left(1 + \left[\frac{m_0 c}{p} \right]^2 \right)^{\frac{1}{2}}$$

Note that this relation is always greater than $1/c$. It is impossible for a freely moving particle to radiate, since for conservation of momentum in this relation conservation of the energy between the particle and the field must be sacrificed. The greatest momentum

for a given amount of energy must be in the direction of energy flow and cannot exceed a ratio of $1/c$.

These relations have been developed for a charged particle freely moving in space. If other matter is present and can take up the excess momentum then the situation would be changed. Such a system can be considered in a dielectric media having the following properties:

$$\epsilon > \epsilon_0$$

$$k > 1$$

$$\mu = \mu_0$$

Assume that the particle has dimensions which are small with respect to the emitted wave lengths, then a particle with charge e , moving in the "z" direction, with speed v , and passing the origin at $t = 0$ has a current density function as follows:

$$J_x(\vec{r}, t) = J_y(\vec{r}, t) = 0$$

$$J_z(\vec{r}, t) = ev\delta(x)\delta(y)\delta(z-vt)$$

where δ = Dirac delta function.

$$\delta(x) = 0 \quad x \neq 0$$

$$\int \delta(x) dx = 1$$

Taking the Fourier integral of the current density, an expression is obtained for the current density which is harmonically dependent upon the time and has amplitude:

$$\bar{J}_z(\vec{r}) = \frac{e}{2\pi} \delta(x)\delta(y) \exp\left[\frac{i\omega z}{v}\right]$$

Since \bar{E} and \bar{H} have a linear dependence upon \bar{J} through Maxwell's

equations, the Poynting vector may be determined for this system as:

$$\bar{P} = \bar{E} \times \bar{H} = \frac{c}{4\pi} \int_0^\infty \int_0^\infty \left[\bar{E}_\omega(\mathbf{r}) \times \bar{H}_{\omega'}(\bar{\mathbf{r}}) e^{-i(\omega+\omega')t} + \bar{E}_\omega^*(\mathbf{r}) \bar{H}_{\omega'}^*(\bar{\mathbf{r}}) e^{i(\omega+\omega')t} + \bar{E}_\omega(\mathbf{r}) \times \bar{H}_{\omega'}^*(\bar{\mathbf{r}}) e^{-i(\omega-\omega')t} + \bar{E}_\omega^*(\mathbf{r}) \times \bar{H}_{\omega'}(\bar{\mathbf{r}}) e^{i(\omega-\omega')t} \right] d\omega d\omega'$$

From this expression the spectral energy distribution can be determined. In order to determine the spectral distribution in frequency, it is necessary to integrate this expression over time from $-\infty$ to $+\infty$ to obtain:

$$P = \frac{c}{4\pi} \int_{-\infty}^{\infty} \left[\bar{E}(\bar{\mathbf{r}}, t) \times \bar{H}(\bar{\mathbf{r}}, t) \right] dt$$

$$P = \frac{1}{2} c \int \left[\bar{E}_\omega(\mathbf{r}) \times \bar{H}_\omega^*(\bar{\mathbf{r}}) + \bar{E}_\omega^*(\mathbf{r}) \times \bar{H}_\omega(\bar{\mathbf{r}}) \right] d\omega$$

$$\bar{P} = 2\pi \bar{P}_\omega(\bar{\mathbf{r}}) \quad (90)$$

Note that $2\pi \bar{P}_\omega(\bar{\mathbf{r}})$ is the flow of energy per unit area in the frequency band of ω to $\omega + d\omega$.

For the system under consideration c may be replaced by $c/\epsilon^{\frac{1}{2}} = c/n$ where n is the refractive index of the media and k may be replaced with nk in the following general expression for Poyntings vector in the z direction.

$$P_z^2 = \frac{k^2}{2\pi r^2 c} \left(\left| \int J_x e^{-ikz'} dt' \right|^2 + \left| \int J_y e^{-ikz'} dt' \right|^2 \right)$$

which has an average energy flux in the direction \bar{k} of:

$$\frac{k^2}{2\pi r^2 c} \left(\left| \int J_{\perp \bar{k}}(\bar{\mathbf{r}}') \left[\exp(-i\bar{k} \cdot \bar{\mathbf{r}}') \right] dt' \right|^2 \right)$$

where $J_{\perp \bar{k}}$ is the component of J perpendicular to the direction \bar{k} .

After making the indicated substitutions for c and k , a value for

$2\pi\bar{P}_{k\omega}(\vec{r})$ may be determined as follows:

$$2\pi\bar{P}_{k\omega}(\vec{r}) = \frac{Ne^2\omega^2 \sin^2\Theta}{4\pi^2 c^3 r^2} \left| \int \left[\exp \left\{ i\omega z' \left(\frac{1}{v} - \frac{N \cos\Theta}{c} \right) \right\} \right] dz' \right|^2$$

where Θ is the polar axis of observation with respect to the z axis

with $J_{\vec{k}} = J_{z\omega} \sin\Theta$, and $\vec{k}\cdot\vec{r} = \bar{k}z' \cos\Theta$.

Evaluating the squared integral, an expression of the form:

$$\frac{4 \sin^2\Theta \left[\frac{1}{2}\omega L \left(\frac{1}{v} - \frac{N \cos\Theta}{c} \right) \right]}{\omega^2 \left(\frac{1}{v} - \frac{N \cos\Theta}{c} \right)^2}$$

is obtained.

Where L is equal to the length of radiation of the particle's path. This expression has a singularity which is a real pole at:

$$\cos\Theta = \frac{c}{Nv} \quad (91)$$

The radiation appears as a cone in the direction of particle movement with a half angle determined by $\frac{c}{Nv}$.

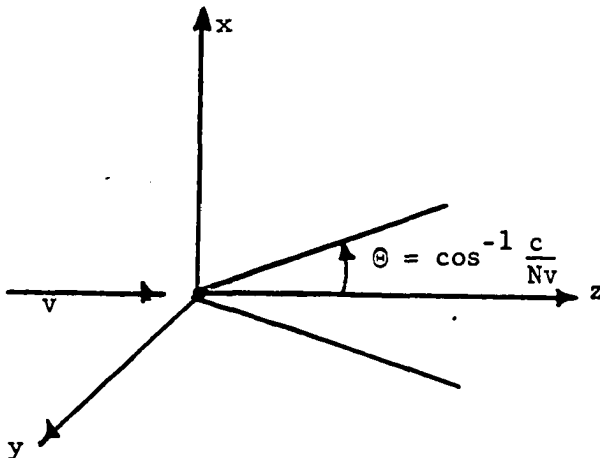


Figure 30

Black Body (9, 25)

It is well known that all objects not at zero temperature radiate energy in the form of electromagnetic waves. Such emission is not in general a major concern in low frequency detecting systems.

A body heated to a temperature T , where T is greater than absolute zero, will radiate energy at a rate proportional to the fourth power of the temperature.

$$E = \sigma T^4 \quad (92)$$

where E = radiated energy

σ = Stefan-Boltzmann constant

T = temperature in degrees Kelvin

Considering a system of harmonic oscillators in thermal equilibrium, where each possesses a single frequency ν , the total energy of each oscillator may be expressed as:

$$U = p^2/2m_0 + 2\pi^2 m_0 \nu q^2 \quad (93)$$

where

p = momentum in generalized coordinates

m_0 = mass of particle

ν = frequency of oscillation

q = displacement in generalized coordinates

U = total energy of the oscillator

In generalized coordinates (p, q) , note that this is the equation for an ellipse. Since U can have only discrete values, then each energy term U defines a new and distinct ellipse in phase space. The important parts of the ellipse are denoted by:

$$a = (2mU)^{\frac{1}{2}} \text{-----semi-major axis} \quad (94)$$

$$b = (U/2\pi^2 m\nu^2)^{\frac{1}{2}} \text{ semi-minor axis} \quad (95)$$

$$A = \pi ab = U/\nu \text{--- area} \quad (96)$$

Re-writing expression (87) to define a new energy equation gives:

$$U = A\nu \quad (97)$$

From quantum theory considerations U may only change by discrete amounts proportional to h ; therefore, the area change due to a jump from one ellipse to another may now be satisfied by h . Since the total energy must be in the form of a series expression with each term separated by a value h , the energy of the n^{th} ellipse is given by:

$$U_n = nh\nu$$

where

$h = \text{Planck's constant}$

Utilizing the Boltzman weighting factor to determine the energy of n oscillators gives:

$$U = h\nu \frac{\sum_{n=0}^{\infty} n \exp(-nh\nu/kt)}{\sum_{n=0}^{\infty} \exp(-nh\nu/kt)} \quad (98)$$

$$U = \frac{h\nu}{\exp(h\nu/kt) - 1} \quad (99)$$

Now within a volume, V , large compared to the wavelength, the number of vibrations in the frequency band ν to $\nu + d\nu$ is given by:

$$dn = \frac{8\pi \nu^2 V}{2} d\nu \quad (100)$$

for V in the shape of a parallel piped.

The density of radiant energy in the enclosure is then given as:

$$\rho_{\nu} = \frac{8\pi h \nu^3}{c^3 (\exp(h\nu/kt) - 1)}$$

This expression is known as Planck's radiation equation. To place this expression in the form of a spectral emissive power expression it is necessary only to note that:

$$E_{\nu} = \frac{\rho_{\nu}}{4} \quad (101)$$

therefore

$$E_{\nu} = \frac{C_1 \nu^3}{c^3 (\exp(h\nu/kt) - 1)} \quad (102)$$

where

$$C_1 = 2\pi^5 h^6 / 15c^3$$

for a parallelepiped.

Now for a radiation into a unit solid angle normal to a Lambert surface $C_1 = 2c^2 h$ and equation (93) may be written as

$$E = \frac{2h\nu^3}{c (\exp(h\nu/kt) - 1)} \quad (103)$$

Now (103) may be utilized to determine the equivalent temperature for a given spectral emission at a known frequency.

APPENDIX C

Recurrence Rate Data

The data utilized to obtain the correlation coefficient is presented in this Appendix in Table 5. Table 6 presents a summary of the reduced repetition rates as determined from the electronic counter for the correlation coefficient calculations.

TABLE 5

RECURRENCE RATE DATA

Exterior Probe x-600	Probe 0.1x	Exterior Probe x-600	Probe 0.1x	Exterior Probe x-600	Probe 0.1x
-71	-7	10	1	31	3
-62	-6	10	1	31	3
-57	-6	12	1	32	3
-52	-5	12	1	32	3
-42	-4	13	1	32	3
-32	-3	13	1	32	3
-29	-3	13	1	34	3
-28	-3	14	1	34	3
-20	-2	14	1	37	4
-16	-2	14	1	40	4
-15	-2	15	2	42	4
-14	-1	15	2	43	4
-14	-1	15	2	44	4
-12	-1	15	2	46	5
-12	-1	17	2	47	5
-9	-1	17	2	650	6
-6	-1	12	2	650	6
-5	-1	18	2	650	6
-4	0	19	2	651	6
-3	0	19	2		
-3	0	19	2		
-2	0	21	2		
0	0	21	2		
0	0	21	2		
0	0	22	2		
+2	0	22	2		
+3	0	23	2		
+4	0	23	2		
+4	0	23	2		
5	1	25	3		
5	1	26	3		
6	1	26	3		
6	1	26	3		
6	1	26	3		
6	1	27	3		
6	1	27	3		
7	1	27	3		
7	1	28	3		
8	1	28	3		
8	1	28	3		
8	1	28	3		
8	1	29	3		
9	1	29	3		
9	1	20	3		
9	1	30	3		

TABLE 5 (Continued)

Interior Probe		Interior Probe		Interior Probe	
y-550	0.ly	y-550	0.ly	y-550	0.ly
-72	-7	-5	-1	27	3
-71	-7	-4	0	28	3
-69	-7	-4	0	28	3
-58	-6	-4	0	30	3
-57	-6	-3	0	32	3
-54	-5	-2	0	32	3
-53	-5	0	0	33	3
-45	-5	0	0	34	3
-45	-5	0	0	36	4
-41	-4	0	0	39	4
-38	-4	1	0	39	4
-37	-4	1	0	47	5
-34	-3	1	0	65	7
-34	-3	3	0		
-28	-3	4	0		
-24	-2	4	0		
-24	-2	4	0		
-24	-2	5	1		
-23	-2	5	1		
-23	-2	6	1		
-21	-2	7	1		
-19	-2	8	1		
-19	-2	9	1		
-16	-2	9	1		
-16	-2	10	1		
-16	-2	12	1		
-15	-2	12	1		
-15	-2	13	1		
-15	-2	14	1		
-15	-2	14	1		
-14	-1	14	1		
-14	-1	15	2		
-13	-1	15	2		
-12	-1	17	2		
-12	-1	18	2		
-11	-1	18	2		
-10	-1	18	2		
-10	-1	20	2		
-10	-1	20	2		
-8	-1	20	2		
-7	-1	20	2		
-7	-1	23	3		
-7	-1	23	3		
-6	-1	23	3		
-6	-1	26	3		

TABLE 6

Summary of Recurrence Data

(0.1x)	N	T	(0.1y)	N	T
± 7	1	49	± 7	4	196
± 6	6	216	± 6	2	72
± 5	3	75	± 5	5	125
± 4	6	96	± 4	6	96
± 3	24	216	± 3	15	135
± 2	22	88	± 2	25	100
± 1	30	30	± 1	30	30
0	11	0	± 0	16	0
	<hr/>	<hr/>		<hr/>	<hr/>
	103	770		103	754

$$\sum x = 128$$

$$\sum xy = 625$$

$$\sum y = -26$$